CO2MVS RESEARCH ON SUPPLEMENTARY OBSERVATIONS



D1.3 Validation of the spatio-temporal characterisation of prior emissions and recommendations for improvement

Due date of deliverable	31/07/2025
Submission date	31/07/2025
File Name	CORSO-D1.3-V1.1.docx
Work Package /Task	WP1/T1.3
Organisation Responsible of Deliverable	BSC
Author name(s)	Marc Guevara ¹ , Oscar Collado ¹ , Gerrit Kuhlmann ² , Erik Koene ² , Stijn Dellaert ³ , Claire Michaud van der Wal ³ , Hugo Denier van der Gon ³ ¹ BSC ² EMPA ³ TNO
Revision number	V1.1
Status	final
Dissemination Level /	PU
location	www.corso-project.eu



The CORSO project (grant agreement No 101082194) is funded by the European Union.

Views and opinions expressed are however those of the author(s) only and do not necessarily reflect those of the European Union or the Commission. Neither the European Union nor the granting authority can be held responsible for them.

1 Executive Summary

This document presents the results derived from intercomparing the global bottom-up point source catalogue developed as part of CORSO T1.2 against a collection of TROPOMI satellite-based (top-down) emission products estimated in CORSO T2.1, including lists of global NO₂ hot spots, NO_x and CO annual estimates from individual industrial plumes and plant-level daily variations of NO_x emissions. The validation process performed in this work allowed to flag inconsistencies between the bottom-up and top-down estimates, and to identify paths for improvements and for a progressive convergence among the inventories, hence reducing the number of flagged inconsistencies. As a result of this validation process, we enhanced the quantification of emissions and addressed misallocations and the inclusion of missing facilities in the bottom-up emission catalogue, reducing the gap with the satellitebased estimates and demonstrating the added value of integrating bottom-up and top-down emission estimation methodologies. A revised version of the bottom-up point source catalogue was produced and is reported as part of the present deliverable. This new version of the catalogue replaces the previous one produced as part of D1.2. A series of recommendations for future improvements of the prior emission catalogue and the top-down emission estimation methods were also identified.

CORSO

Table of Contents

1	Exec	utive Summary	2
2	Intro	duction	4
	2.1	Background	4
	2.2	Scope of this deliverable	4
	2.2.1	Objectives of this deliverable	4
	2.2.2	Work performed in this deliverable	5
	2.2.3	Deviations and counter measures	5
	2.3	Project partners:	6
3	Inter	comparison between bottom-up and top-down industrial emission estimates	7
	3.1	Consistency between NO _x industrial hotspot locations	7
	3.1.1	Bottom-up geographical locations	7
	3.1.2	Top-down hotspot locations	7
	3.1.3	Results of the intercomparison	9
	3.2	Consistency between annual NO _x emissions	12
	3.2.1	Bottom-up emission estimates	12
	3.2.2	Top-down emission estimates	12
	3.2.3	Results of the intercomparison	13
	3.3	Consistency between annual CO emissions from iron and steel plants	21
	3.3.1	Bottom-up emission estimates	21
	3.3.2	Top-down emission estimates	21
	3.3.3	Results of intercomparison	24
	3.4	Daily variations of NO _x emissions	31
	3.4.1	Bottom-up emission estimates	31
	3.4.2	Top-down emission estimates	31
	3.4.3	Results of the intercomparison	31
4	Revi	sed version of the CORSO point source catalogue	32
	4.1	Impact on the bottom-up emission estimates	32
	4.2	Impact on the consistency with top-down emission results	34
	4.3	CORSO point source catalogue version 2	37
5	Cond	clusions and recommendations for future improvements	38
6	Refe	rences	41

2 Introduction

2.1 Background

To enable the European Union (EU) to move towards a low-carbon economy and implement its commitments under the Paris Agreement, a binding target was set to cut emissions in the EU by at least 40% below 1990 levels by 2030. European Commission (EC) President von der Leyen committed to deepen this target to at least 55% reduction by 2030. This was further consolidated with the release of the Commission's European Green Deal on the 11th of December 2019, setting the targets for the European environment, economy, and society to reach zero net emissions of greenhouse gases in 2050, outlining all needed technological and societal transformations that are aiming at combining prosperity and sustainability. To support EU countries in achieving the targets, the EU and European Commission (EC) recognised the need for an objective way to monitor anthropogenic CO₂ emissions and their evolution over time.

Such a monitoring capacity will deliver consistent and reliable information to support informed policy- and decision-making processes, both at national and European level. To maintain independence in this domain, it is seen as critical that the EU establishes an observation-based operational anthropogenic CO₂ emissions Monitoring and Verification Support (MVS) (CO2MVS) capacity as part of its Copernicus Earth Observation programme.

The CORSO research and innovation project will build on and complement the work of previous projects such as CHE (the CO2 Human Emissions), and CoCO2 (Copernicus CO2 service) projects, both led by ECMWF. These projects have already started the ramping-up of the CO2MVS prototype systems, so it can be implemented within the Copernicus Atmosphere Monitoring Service (CAMS) with the aim to be operational by 2026. The CORSO project will further support establishing the new CO2MVS addressing specific research & development questions.

The main objectives of CORSO are to deliver further research activities and outcomes with a focus on the use of supplementary observations, i.e., of co-emitted species as well as the use of auxiliary observations to better separate fossil fuel emissions from the other sources of atmospheric CO₂. CORSO will deliver improved estimates of emission factors/ratios and their uncertainties as well as the capabilities at global and local scale to optimally use observations of co-emitted species to better estimate anthropogenic CO₂ emissions. CORSO will also provide clear recommendations to CAMS, ICOS, and WMO about the potential added-value of high-temporal resolution ¹⁴CO₂ and APO observations as tracers for anthropogenic emissions in both global and regional scale inversions and develop coupled land-atmosphere data assimilation in the global CO2MVS system constraining carbon cycle variables with satellite observations of soil moisture, LAI, SIF, and Biomass. Finally, CORSO will provide specific recommendations for the topics above for the operational implementation of the CO2MVS within the Copernicus programme.

2.2 Scope of this deliverable

2.2.1 Objectives of this deliverable

The objective of this deliverable is to intercompare the global bottom-up point source dataset constructed under T1.2 against top-down emission estimates developed in T2.1 with the aim of identifying the main discrepancies between the two datasets, analysing and discussing the main drivers behind them and, when possible, reducing them. We also provide recommendations for future improvements of the prior emission catalogue and the top-down emission estimation methods.

2.2.2 Work performed in this deliverable

The intercomparison work performed focusses on three topics:

- <u>Topic 1 Consistency between top-down and bottom-up hotspot locations</u>: TROPOMI-based lists of NO₂ hotspot locations are compared with the geographical locations reported in the bottom-up global point source database (section 3.1)
- Topic 2 Consistency between top-down & bottom-up annual emissions: Annual TROPOMI-based NO_x and CO emissions for selected industrial hotspots are compared against the estimates provided by the bottom-up point source catalogue (sections 3.2 and 3.3).
- <u>Topic 3 Consistency between top-down & bottom-up emission time series</u>: TROPOMI-based daily NO_x time series from selected industrial point sources are compared against estimates derived from continuous emission monitoring system (section 3.4).

The reference year of the intercomparison exercise is 2021 for all the cases. For each topic, discrepancies between the bottom-up and top-down emission datasets are identified, discussed and, when possible, reduced. The intercomparison work has resulted in an updated version of the bottom-up global point sources catalogue (CORSO point source database version 2), which replaces the previous one produced as part of D1.2 (CORSO point source database version 1). The improvements performed were as follows:

- Correction of the geographical location of plants
- Addition of missing plants
- Update of country- and fuel-dependent NO_x:CO₂ and SO_x:CO₂ emission ratios
- Review split of dual fuel power plants
- Correction of bug associated to the filtering of "operating" units:
- Review geographical location and installed capacity of oil-fired power plants in selected countries

Details of these improvements are provided in Section 4. The updated version of the global point source database is compared against its predecessor to quantify the impact of the implemented improvements on the total annual emissions and their spatial distribution.

Besides incorporating these changes, recommendations for future improvements were also identified and described to continue increasing the robustness and representativity of the prior emission datasets and top-down estimation methods to be used in the future CO2MVS.

2.2.3 Deviations and counter measures

GEMS-based NO_x emission estimates for Southeast Asia were not considered in the intercomparison due to the uncertainties and limitations associated to the current retrievals and subsequent challenges of deriving robust top-down emission estimates. Top-down estimates for this region were derived from TROPOMI observations.

The submission of the deliverable was delayed one month (July 2025 instead of June 2025) to allow finalising the production of all the top-down emission products and having enough time to not only flag inconsistencies with the bottom-up estimates but also identify paths for improvements and for a progressive convergence among the emission estimates. As a result of this extension, we managed to produce a revised and improved version of the bottom-up point source catalogue, which was not originally planned.

2.3 Project partners:

Partners	
EUROPEAN CENTRE FOR MEDIUM-RANGE WEATHER	ECMWF
FORECASTS	
AKADEMIA GORNICZO-HUTNICZA IM. STANISLAWA	AGH
STASZICA W KRAKOWIE	
BARCELONA SUPERCOMPUTING CENTER - CENTRO	BSC
NACIONAL DE SUPERCOMPUTACION	0=4
COMMISSARIAT A L ENERGIE ATOMIQUE ET AUX ENERGIES ALTERNATIVES	CEA
KAMINSKI THOMAS HERBERT	iLab
METEO-FRANCE	MF
NEDERLANDSE ORGANISATIE VOOR TOEGEPAST	TNO
NATUURWETENSCHAPPELIJK ONDERZOEK TNO	
RIJKSUNIVERSITEIT GRONINGEN	RUG
RUPRECHT-KARLS-UNIVERSITAET HEIDELBERG	UHEI
LUNDS UNIVERSITET	ULUND
UNIVERSITE PAUL SABATIER TOULOUSE III	UT3-CNRS
WAGENINGEN UNIVERSITY	WU
EIDGENOSSISCHE MATERIALPRUFUNGS- UND	EMPA
FORSCHUNGSANSTALT	
EIDGENOESSISCHE TECHNISCHE HOCHSCHULE ZUERICH	ETHZ
UNIVERSITY OF BRISTOL	UNIVBRIS
THE UNIVERSITY OF EDINBURGH	UEDIN

3 Intercomparison between bottom-up and top-down industrial emission estimates

The following subsections present the results derived from intercomparing the global bottomup point source catalogue developed as part of CORSO T1.2 against a collection of satellitebased emission products estimated in CORSO T2.1 As previously indicated, the intercomparison exercises focusses on three aspects:

- Topic 1 Consistency between top-down and bottom-up hotspot locations
- Topic 2 Consistency between top-down & bottom-up annual emissions
- Topic 3 Consistency between top-down & bottom-up emission time series

For each topic, discrepancies between the bottom-up and top-down emission datasets are identified and discussed. The actions taken to reduce these discrepancies are also described when applicable. Key elements of the bottom-up and top-down estimation methods are briefly described at the beginning of each subsection. For a more detailed description of the emission estimation methods considered, we refer to CORSO deliverables D1.2 for the bottom-up point source catalogue and D2.1, D2.2 and D2.3 for the top-down emission estimates.

3.1 Consistency between NO_x industrial hotspot locations

3.1.1 Bottom-up geographical locations

In the CORSO bottom-up point source catalogue, information on the geographical location of each individual industrial plant is obtained from multiple datasets, including the integrated Industrial Reporting Database (EEA, 2024) for European facilities and a mosaic of data sources for non-European industries, namely: the Global Energy Monitor trackers (GEM), the Emissions and Generation Resource Integrated Database (eGRID) and the ClimateTRACE database (Sinha and Crane, 2024).

For both the European and non-European databases, substantial effort was put into identifying missing and incorrect facility coordinates under the framework of T1.2. For Europe, at least the top 100 facilities (in terms of CO₂ emissions) were manually checked. In addition, visual inspection of plotted maps to identify emission locations in illogical places (e.g. outside Europe, in the sea, or in the wrong country) was used to check and correct obvious errors. For the non-European dataset, the review process was performed for those GEM facilities for which the precision of their coordinates is identified as "approximate" and that have a capacity larger than 300MW.

It is important to note that the coverage of small power and heat plants is relatively poor in the bottom-up catalogue. In Europe, the facility-level reporting in the integrated Industrial Reporting Database is dependent on both emission level thresholds (e.g. 100 kton CO_2 /year) or plant thermal input capacity thresholds (> 50 MW thermal), leading to smaller plants being omitted from the inventory. A similar situation occurs for non-European power plants, with units with capacities < 50 MW thermal not being considered due to lack of data.

3.1.2 Top-down hotspot locations

Two lists of TROPOMI-based NO₂ hotspots locations were developed as part of T2.1 using two independent methods.

Method 1: The Getis-Ord Gi* statistic method (Getis and Ord, 1992; Caliskan and Anbaroglu, 2023) was used to compute TROPOMI-based NO₂ hotspots as described in D2.1. This method characterize hotspots using two key statistical metrics: Gi* (Getis-Ord statistic) and the p-value. Gi* measures the degree of spatial clustering, indicating how much a given point stands out relative to its surroundings. Higher values reflect stronger clustering of high NO₂ concentrations, making the point more relevant as a potential hotspot. The p-value, on the

other hand, assesses the statistical significance of the hotspot, with lower values indicating a higher probability that the point is not a result of random variation. Given that the initial list of hotspots consisted of approximately 80,000 points (green dots in Figure 1), a filtering strategy was necessary to focus on the most relevant hotspots. To achieve this, we applied a series of selection criteria to reduce the dataset while maintaining its significance and reliability. The first filter was based on statistical significance. We retained only the points where Gi* was greater than or equal to 1.96 and the p-value was less than or equal to 0.05. According to D2.1, this threshold corresponds to the 95th percentile of the data, ensuring that only the most statistically significant and spatially clustered hotspots were considered. This step eliminated points with weak clustering or insufficient statistical confidence, allowing us to focus on the most relevant locations. In addition to statistical filtering, two spatial exclusion criteria were applied to remove points that might be influenced by major urban centers or localized emission sources. The first spatial filter excluded any hotspot located within 15 km of a city classified as rank 1 or rank 2, as reported by the ESRI World urban areas. These cities typically exhibit high NO₂ levels due to traffic density and industrial activity, which could interfere with the identification of more isolated hotspots. By removing these areas, the analysis focused on regions where NO₂ concentrations were less likely to be dominated by large-scale urban pollution. The second spatial filter targeted known industrial emission sources. Specifically, we removed any hotspot located within 15 km of a point source from the CORSO bottom-up catalogue, since we are particularly interested in identifying potential hotspots that have not been well characterized in this dataset. As a result of applying these filtering steps, the dataset was reduced to approximately 30,000 points (blue dots in Figure 1), However, regions such as the USA, Europe, China and the area between Congo and Angola are still densely populated with points after applying the filer, making it difficult to distinguish individual hotspots. For the rest of the world, a detailed manual selection of the filtered NO₂ hotspots was performed (yellow dots in Figure 1), taking into account those hotspots for which no bottom-up point source was located nearby. The analysis of these locations led to several modifications in the bottom-up catalogue, as described in subsection 3.1.3.



Figure 1 Representation of the top-down hotspots locations estimated with method 1. The green dots represent all the identified hotspots, while the blue points correspond to those that were filtered based on statistical and spatial criteria. The yellow points indicate the manually selected hotspots of interest for further analysis.

Method 2: Annual average emission fields were computed using the divergence method (see D2.2 and Section 3.2.2 for details). This approach integrates TROPOMI NO₂ satellite observations with ERA5 wind fields to derive high-resolution global maps of emission fluxes at 0.03° (approximately 3 km) spatial resolution. Note that the resulting map of emission fluxes (units of kg/m2/s) itself is computed on each individual TROPOMI overpass before regridding, so we're not interpolating the "raw" TROPOMI data but a derived product. Therefore, we're not artificially increasing the native resolution of the TROPOMI observations (5.5km x 3.5 km) but just storing them on a finer grid for accumulation/averaging of the data. The regridding process is performed using a conservative remapping approach, we consider the fractional overlap between TROPOMI pixels and the fine output grid to perform the remapping.

Compared to simple averaging of satellite images, the divergence method offers improved spatial differentiation of emission sources. However, it is sensitive to artefacts, particularly in regions with complex topography, due to the numerical differentiation involved in flux calculations. To better identify point sources, we therefore applied a topography correction that subtracts the product of annual mean wind speed and annual mean gradient of the NO₂ field.

To compare bottom-up and top-down locations of point sources, the CORSO point source database was overlayed with TROPOMI emission map using GoogleEarth Engine. The maps were visually inspected to identify deviation between bottom-up and top-down source locations in Africa (Figure 2), America, and Europe.

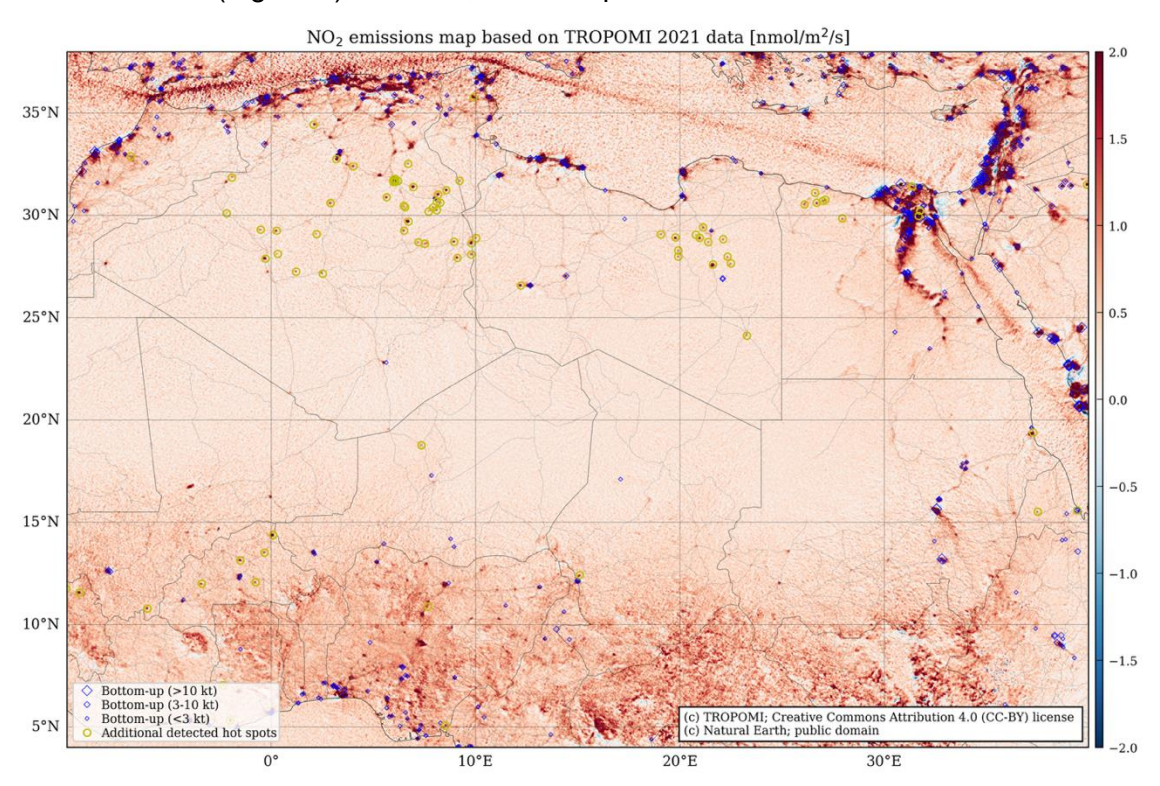


Figure 2 TROPOMI-based NO₂ hotspot locations against locations of industrial point sources as reported by the CORSO bottom-up catalogue in Northern Africa. The yellow circles indicates TROPOMI-based detected hotspots not reported in the bottom-up catalogue.

3.1.3 Results of the intercomparison

The comparison between top-down and bottom-up industrial hotspot locations described previously in sections 3.1.1 and 3.1.2 resulted in the following findings and modifications of the CORSO bottom-up point source catalogue:

- <u>Correction of location of plants:</u> Geographical locations for a total of 41 plants were corrected. These corrections were made in Lebanon, Brazil, Venezuela, Spain, Africa, Saudi Arabia, Pakistan, Iraq and Bangladesh.
- Addition of missing plants: A total of 8 unlisted facilities were added to the revised version of the bottom-up catalogue. For most of the cases (5 out of 8), the added plants were small and isolated power plants with installed capacities below 50 MW (e.g., Pribbenow power plant in Colombia, with an installed capacity of 12.7MW). These facilities were not previously included either because they are below the capacity threshold considered by the data sources used in the catalogue (see section 3.1.1) or because they were located in countries not included in the International Energy Agency (IEA) energy statistics (i.e., Timor-Leste, Guinea), which are used as input to estimate the bottom-up emissions. For the countries missing in the IEA statistics, emissions where estimated using the energy statistics provided by the <u>US Energy Information Administration (EIA)</u>. Three missing large point sources were also included during this process, namely the Kosovo A and B lignite-fired power stations (Figure 3) and the Secunda synthetic fuel plant, located in South Africa.
- <u>Identification of additional large emitting industrial sources:</u> A manual inspection revealed other strong emission sources observed by TROPOMI and that are currently not included in the bottom-up catalogue, mainly refineries and mining activities (e.g., copper smelters, cobalt refineries). These facilities were mainly identified across North Africa (refineries) as well as in Chile, Peru, Zambia, and the Democratic Republic of the Congo (mining activities; Figure 4), the findings being in line with other recently published works (e.g., Martínez-Alonso, 2023).

CORSO point source catalogue version 1 CORSO point source catalogue version 2

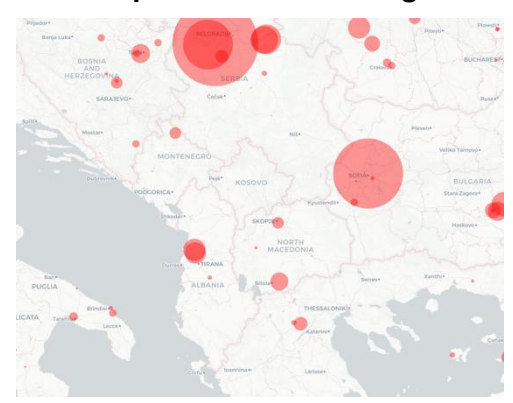




Figure 3 Plant-level annual NO_x emissions (kt/year) reported by the CORSO global point source database versions 1 and 2 over Eastern Europe.

CORSO

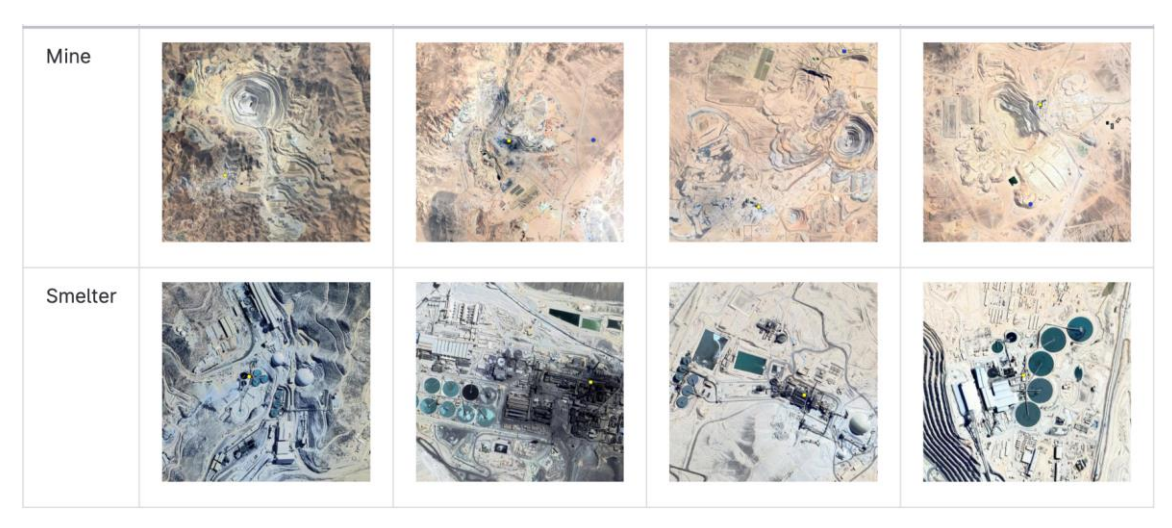


Figure 4 Examples of copper mines (first row) and associated copper smelters (zooms, yellow dots) identified in Chile using the top-down NO_2 hotspot locations

3.2 Consistency between annual NO_x emissions

3.2.1 Bottom-up emission estimates

For European plants, annual bottom-up emissions were mainly derived from the EU integrated Industrial Reporting Database, combining both the facility- and plant-level data into one location total. Plant-specific emissions for all US power plants were obtained from the official eGRID database. For the rest of the world, emissions per plant were estimated by first combining activity factors and CO₂ emission factors at the national level and then spatially distributing emission across facilities considering their characteristics (fuel used and installed capacity). Estimation of annual NO_x emissions were obtained by combining the CO₂ annual estimated emissions with fuel- and country-dependent average emission ratios. For more details on the description of the bottom-up estimation methodologies and sources of information considered, we refer to CORSO D1.2.

3.2.2 Top-down emission estimates

 NO_x emissions from point sources were estimated from TROPOMI NO_2 observations using the divergence (DIV) method and the cross-sectional flux (CSF) method, which are described in CORSO Deliverable D2.2 in detail:

- The **divergence method (DIV)** computes the emission field F from the divergence of the flux and the sink term that account for NO_x decay (F=∇·(*Ū* VCD)+VCD/τ), where U is the wind vector from the ERA5 reanalysis product, VCD is the tropospheric NO₂ vertical column density and τ is the lifetime (tau = 4 hours). The flux field is computed for each satellite swath and then averaged on a global grid of 0.03 degrees. The NO_x emissions of a source are computed by integrating the NO₂ emission field in a circle around the source, which is chosen to only include the local enhancement (see Figure 5 for illustration). Finally, an air mass factor correction is applied, and NO₂ is converted to NO_x using a NO₂-to-NO_x conversion factor (f = 1.65 + 0.5 VCD/VCDmax). Monthly and annual emissions were computed for a total of 173 point sources in the CORSO point source database.

Source Analysis: Kraftwerk Boxberg (Lon: 14.57, Lat: 51.42, AMF correction: \times 1.49, NO2 \rightarrow NOx: \times 1.74)

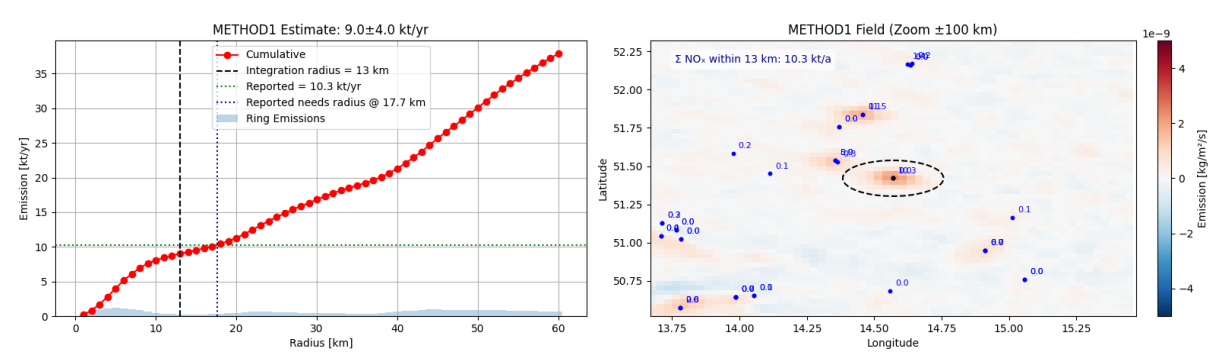


Figure 5 TROPOMI-based annual NO_x emissions for the Kraftwerk Boxberg power plant (Germany) using the divergence method. Integration radius is defined by checking the curvature of the radial profiles and selecting the point that maximally contains the source without including the next one.

- The cross-sectional flux (CSF) method estimates emissions from point sources for each TROPOMI satellite overpass. It begins by identifying the plume area, which is defined as a region extending up to 30 km downwind and 60 km across, based on the ERA5 wind vector. A Gaussian curve with a linear background is fitted to the plume to obtain the NO₂ line density *q* from which the NO₂ flux is computed using the ERA-5 wind speed. Air mass factors are computed using the averaging kernels and a

modified NO $_2$ profile that includes the local enhancement. To account for NO $_2$ to NO $_x$ conversion f and NO $_x$ lifetime τ , we used the machine-learning model trained with GEOS-Chem data for Europe (Schooling et al. 2025) and default values otherwise (f = 1.32 and τ =4 hours). Emissions were estimated for the TOP 100 sources in the CORSO point source database and 21 iron and steel (I&S) plants in Europe. The estimates are quality filtered by removing estimates where the standard width or the shift of the Gaussian curve is larger than 10 km and where wind speeds are smaller than 2 m/s and larger than 10 m/s. Figure 6 shows an example of the CSF method applied to a TROPOMI NO $_2$ image containing the emission plume of the U.S. New Madrid Power Plant.

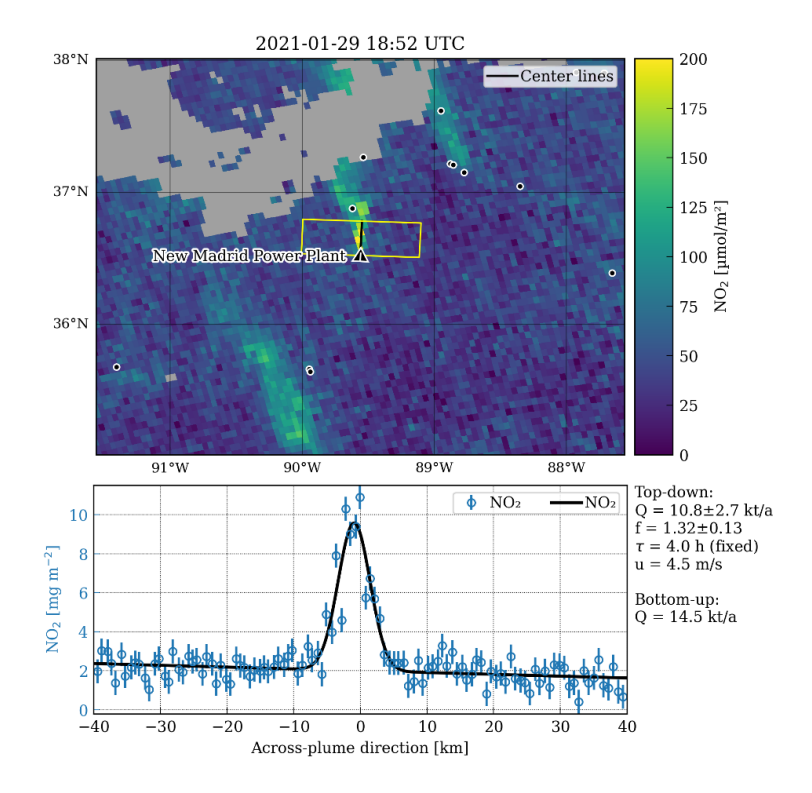


Figure 6 Example of the CSF method applied to estimate NO_x emissions from the New Madrid Power Plant in the USA. (upper) TROPOMI NO_2 image on 29 January 2021 (18:52 UTC) with plume region marked by yellow polygon. (lower) Across-plume columns in across-plume direction with Gaussian curve fitted to estimate line densities. Emission rate (Q) is computed from line density and wind speed (u=4.5 m/s) using a NO_2 -to- NO_x conversion factor (f=1.32) and a NO_x lifetime (τ) of 4 hours. In this example, the NO_x emission rate at overpass was estimated as 10.8 kt NO_2 / a, while the bottom-up inventory states an annual mean emission of 14.5 kt/a.

3.2.3 Results of the intercomparison

Four filtered versions of the original CORSO bottom-up point source database were produced to select optimal targets for the bottom-up versus top-down plant-level intercomparison exercise. These filtered catalogues were constructed considering the following criteria:

- Top 100 NO_{x} emitting plants with annual NO_{x} emissions equal or higher than 3kt/year, this value being defined as the minimum threshold for TROPOMI to detect and quantify emitters.
- Top 100 NO_x emitting plants with annual NO_x emissions equal or higher than 3kt/year, including at least 10 plants in EU27+UK, 10 plants in the USA and a maximum of 5 plants in each one of the other countries.

- Top 100 NO_x emitting plants with annual NO_x emissions equal or higher than 3kt/year, excluding those that are within 10 km of a city classified as rank 1 or 2 by the <u>ESRI</u> World urban areas.
- Top $100~\text{NO}_x$ emitting plants with annual NO_x emissions equal or higher than 3kt/year, including at least 10 plants in EU27+UK, 10 plants in the USA and a maximum of 5 plants in each one of the other countries, and excluding plants that are within 10 km of a city classified as rank 1 or 2 by the ESRI World urban areas.

The combination of the four filtered catalogues resulted in a list of 173 individual plants for which top-down estimates were produced following the DIV method described in Section 3.2.2. It is important to note that all these 173 individual points represented power plants.

Figure 7 to Figure 8 presents the results of the comparison between plant-level annual NO_x emissions estimated by the CORSO bottom-up catalogue (blue) and derived from TROPOMI (orange) using the DIV method for selected countries and regions, including EU27+UK, USA, South Africa, India, Australia, Saudi Arabia and Indonesia. Grey bars represent the bottom-up emissions from other CORSO point sources located within the integration radius considered in the top-down estimates. Black dots highlight those power plants that are within 10 km of a city classified as rank 1 or rank 2 by the ESRI World urban areas. Black lines indicate the uncertainty range associated to the top-down emission estimates. The computation of uncertainties was done with a root sum square approach to combine several error components, all of which include some assumed values (e.g., we assume an error component of 10%*365/valid overpasses, where valid overpasses simply means we only take TROPOMI images with a QA value over 0.75, thus if there are fewer valid overpasses this uncertainty factor increases). The numbers as provided here represent a rough estimate of the 1-sigma uncertainty, acknowledging that the uncertainty itself carries a degree of uncertainty. In rare cases, the uncertainty range extends below zero, particularly in cases where data coverage is sparse. This does not indicate the source may be a sink, but it does indicate the estimate has a 100% uncertainty, which likely over-estimates the uncertainty in such cases. The topic of coming up with reliable uncertainties is a topic of active research

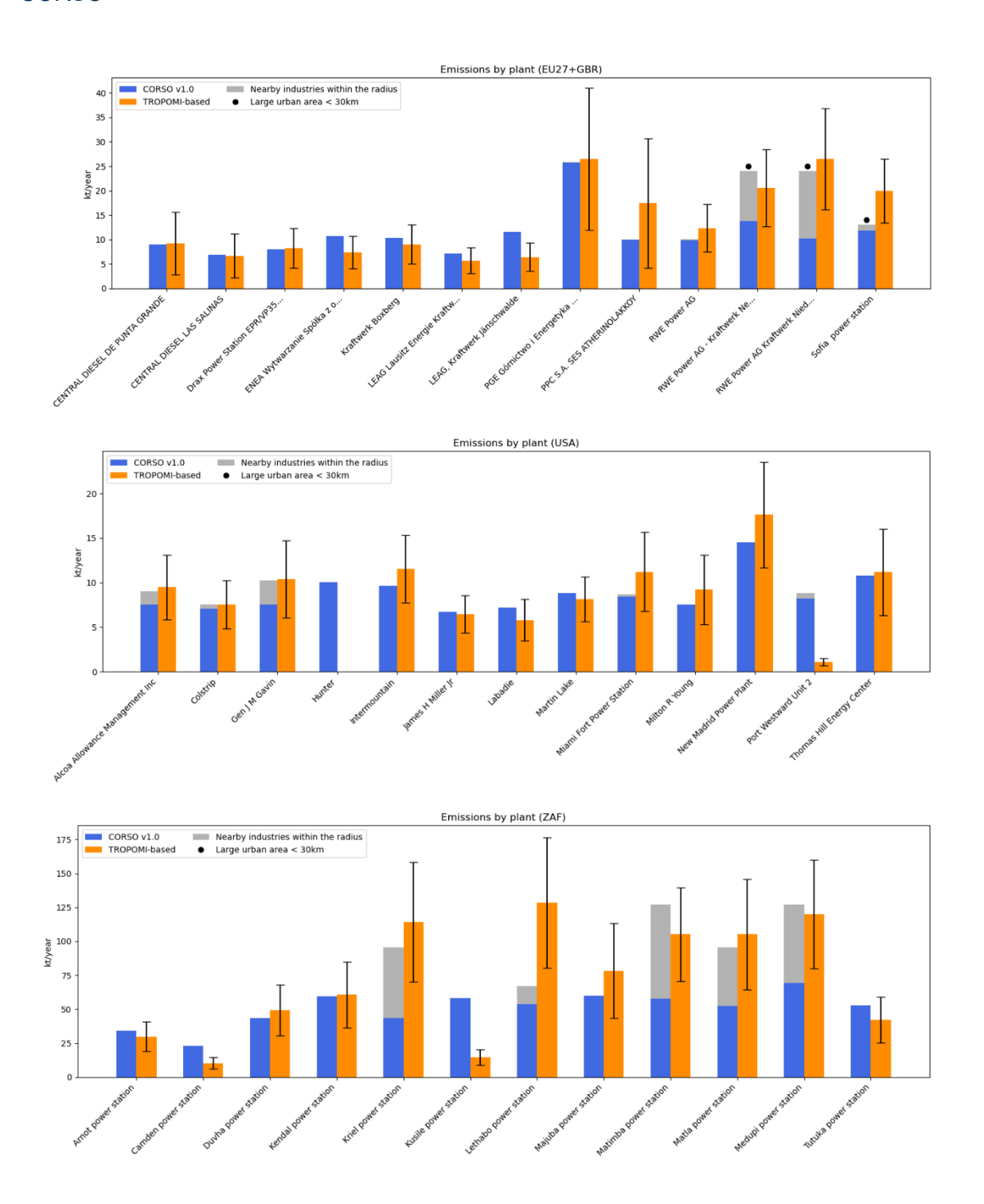
A good agreement between the bottom-up and TROPOMI-based estimates is reported for EU27+UK, USA. The consistency observed in these two regions provides confidence in the top-down results, as the bottom-up emissions are based on the data officially reported by the the EU integrated Industrial Reporting Database and the EPA eGRID database, which for large power plants typically rely on emission monitored data. The DIV method is not reporting emissions for the Hunter power plant in the USA. This is because the automated emission estimation routine for the DIV method failed to find a suitable integration range for this plant due to a big topographic overprint, the plant is located in a valley, and erroneous wind speeds and directions reported by ERA5.

Results also indicate a good match between bottom-up and top-down estimates in countries dominated by coal-fired power plants, such as South Africa, India or Australia, the bottom-up estimates from each plant being generally within the range of uncertainty provided by the top-down results. Despite this general consistency between estimates, important discrepancies can be observed for some individual plants, which can be related to multiple aspects. For instance, large discrepancies are observed for the Kusile and Lethabo power plants in South Africa, the bottom-up estimates being approximately three times larger than the top-down in the first case and two times lower in the second one. For the Kusile power plant, we found out that the CORSO point source catalogue was wrongly including three units that became operational after 2021, which artificially increased its total installed capacity by 50% (2400MW). Since installed capacity is used as a proxy for the spatial distribution of total national emissions across plants, the identified bug was producing an overallocation of emissions in this plant. The bug was corrected in the new version of the catalogue, which led to a reduction of the inconsistencies with the top-down estimates, as described in Section 4. For the Lethabo power plant, we hypothesise that the top-down estimates are influenced by

CORSO

other industrial and anthropogenic sources not reported in the CORSO bottom-up catalogue, as the plant is located in the Vaal Triangle area, a highly industrialised region and one of the most polluted areas in South Africa (Muyemeki et al., 2021).

For some countries such as Saudi Arabia and Indonesia, large discrepancies between the emission estimates are observed across most of the power plants, the bottom-up catalogue generally reporting much larger emissions than the top-down estimates (up to a factor of 5). For the case of Saudi Arabia, the main cause of discrepancies in the emission estimate is the way dual fuel power plants are treated in the CORSO point source database. Our assumption is that all dual-fuel plants in a country use both natural gas and oil, and that the use of each fossil fuel in the plant is proportional to the usages reported by the IEA at the country level. This assumption is proved wrong when comparing the resulting bottom-up estimates against the top-down results, which clearly indicate that some of these dual fuel plants are only operating using natural gas, since estimates emissions are much lower. Based on these results, the hypothesis used to estimate emissions from dual fuel power plants was revised as described in Section 4. For the case of Indonesia, we hypothesise that the large discrepancies between results are related to an overestimation of the NO_x:CO₂ emission ration considered for coal-fired power plants in this country, as later described in Section 4. Note also that some of the bottom-up estimates in Indonesian power plants are affected by the bug in the filtering of operating units described above. This is the case of Bangko Tengah and Central Java power plants, which units started operating in 2023 and 2022, respectively, and therefore TROPOMI-based estimates reported no emissions for these facilities in 2021. For some Indonesian power plants, the range of uncertainty reported by the top-down estimates includes negative emission values (i.e., Sulawesi Labota and Weda Bay power plants). These negative values are expected when using mass-balance approaches, particularly when the estimated value is smaller than the associated uncertainty. We do not remove negative values, just as we do not remove positive ones, because doing so would introduce a bias and lead to an overestimation of emissions.



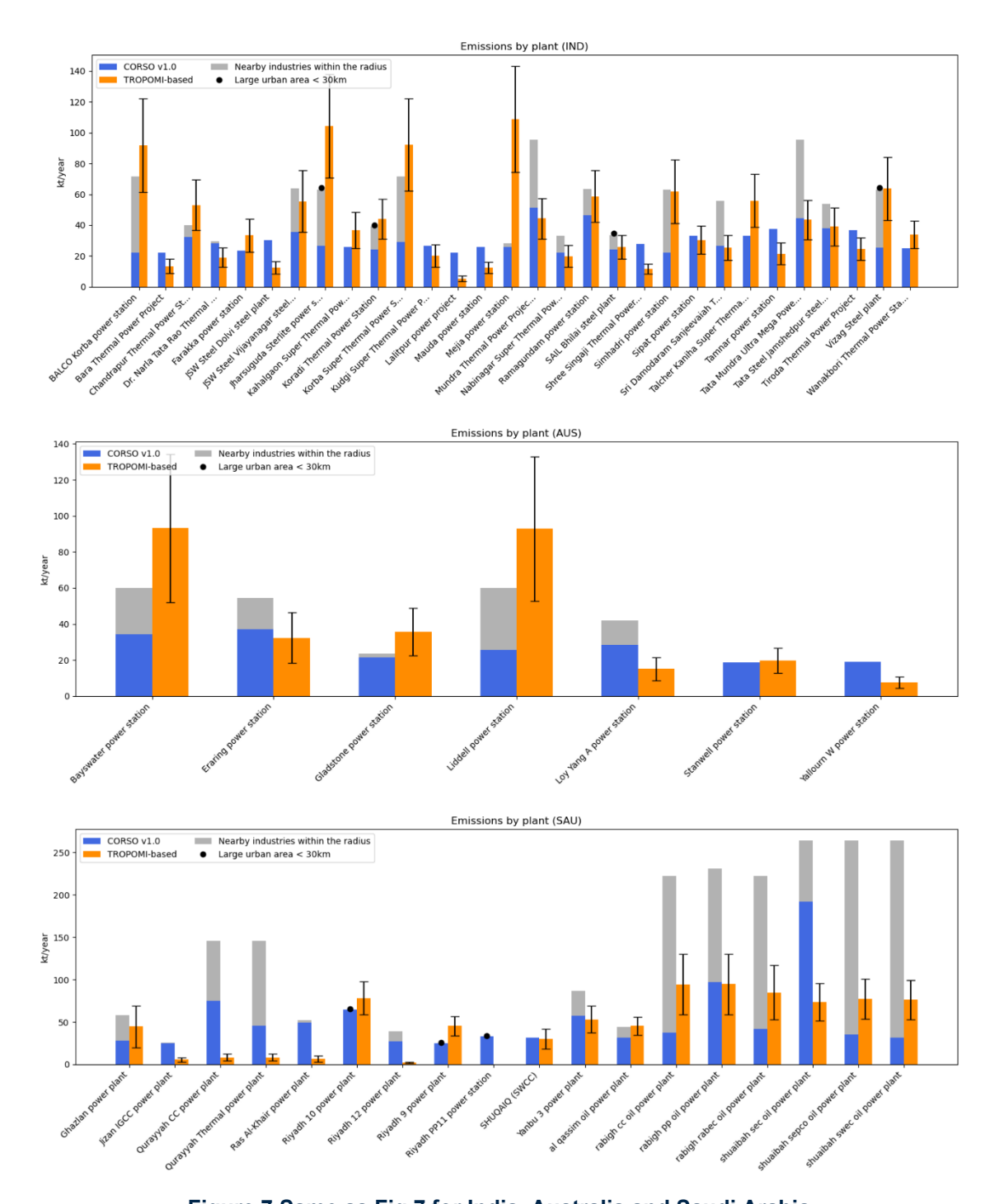


Figure 7 Same as Fig.7 for India, Australia and Saudi Arabia

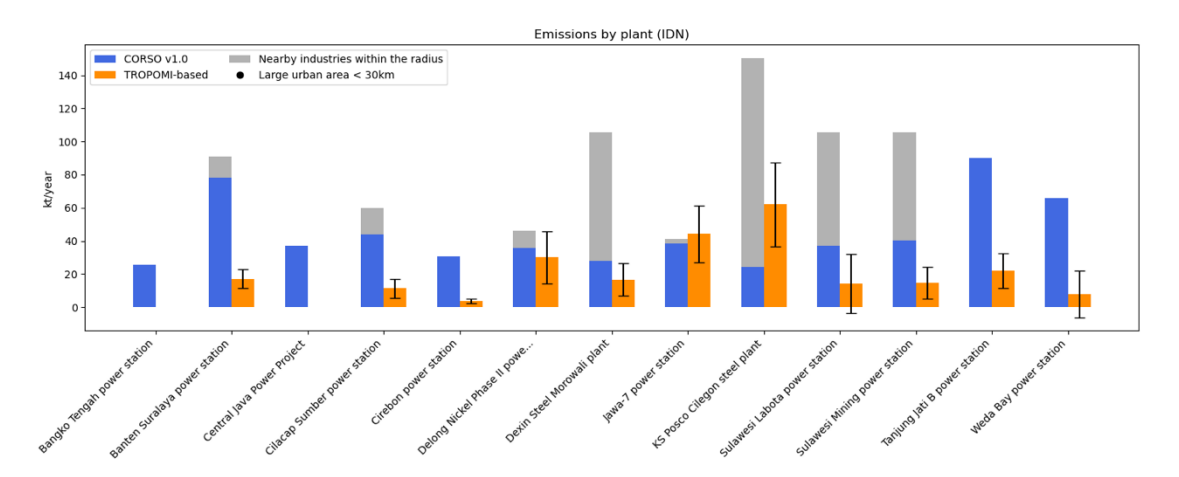


Figure 8 Same as Fig.7 for Indonesia.

Besides the selected optimal targets, a dedicated comparison between bottom-up and top-down plant-level NO_x emission estimates using the CSF method was performed for a total of 20 European I&S plants (Figure 9). This exercise was performed to complement the intercomparison work previously done for CO emissions by Leguijt et al. (2025). These facilities exhibit relatively low NO_x emissions, ranging from 0.6 to 9.8 kt NO_2 per year, with a median of 3.3 kt/a based on the CORSO bottom-up inventory. To quantify the uncertainty in the CSF top-down estimates, we assume a random uncertainty of 30% for individual measurements and an additional 30% to account for temporal sampling bias. A minimum systematic uncertainty of 20% is also applied.

Top-down estimates are compared to bottom-up reports, considering emissions from the I&S plant itself as well as from point sources within 10 km and 30 km radii. We find that top-down estimates significantly exceed bottom-up reports, with mean biases of 3.9 kt/a (114%) and 1.4 kt/a (44%) for the 10 km and 30 km radii, respectively. This result contrasts with the below findings suggesting that assumptions in NO_x chemistry would lead to underestimation in top-down approaches with the CSF method.

The discrepancy likely arises because the bottom-up inventory includes only the largest point sources. I&S plants are often situated in industrial zones, where we expect additional emissions from smaller but numerous sources from other sectors as well as from residential/commercial heating and traffic emission sources. Due to the relatively low emissions from the I&S plants, these surrounding sources may contribute more significantly than in regions dominated by major emitters, such as those identified as part of the Top 100 CORSO NO_x emitting plants.

A second issue is that many emitters are at the detection limit of the TROPOMI instrument, which is likely around 3 kt/year for the CSF method. We therefore only detect plumes when emissions are large. Since the plants will have temporal variability of emissions, including days with zero emissions, we naturally overestimate the emissions.

In conclusion, NO_x emissions from I&S production in Europe are currently at or near the detection limit for satellite instruments like TROPOMI. Future missions such as CO2M, with higher spatial resolution, and facility-scale scanners like TANGO, are expected to improve the detection and quantification of these weaker sources.

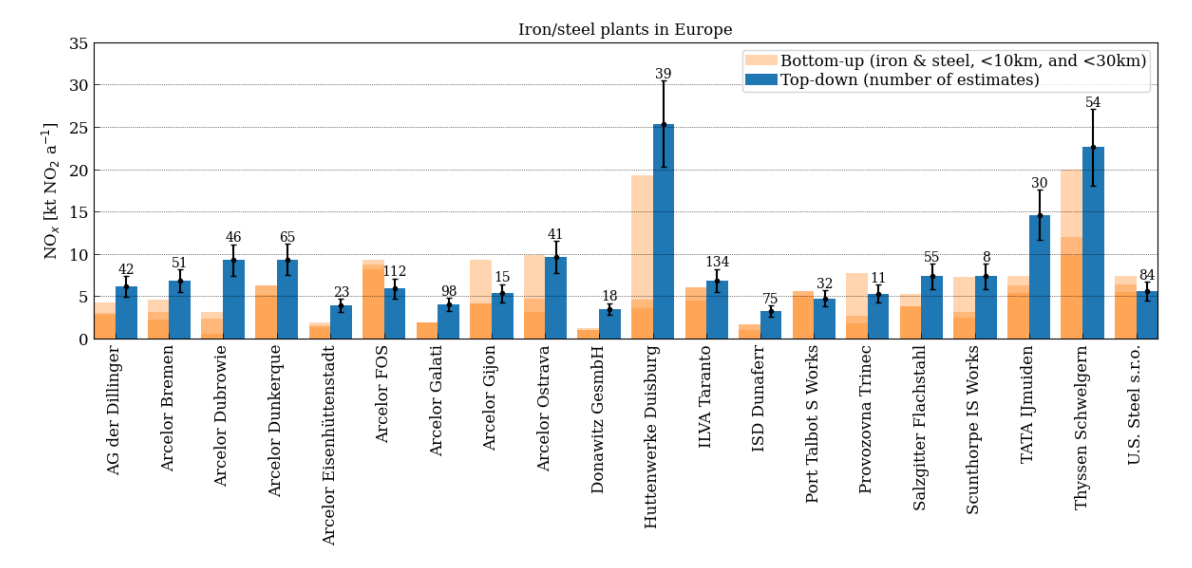


Figure 9 Comparison between annual NO_x emissions of I&S plants between the CORSO bottom-up catalogue and derived from TROPOMI NO_2 observations using the CSF method. Number of top-down estimates per year are indicated for each plant. Bottom-up estimates are shown for I&S plants within 10 km, for all CORSO point sources within 10 km, and for all CORSO point sources within 30 km. The error bars show 1-sigma uncertainty annual emissions, assuming 30% uncertainty of individual estimates, 30% sampling bias, as well as systematic error of at 20% due to NO_x chemistry.

A large uncertainty of the top-down NO_x emission estimates is related to the correction for NO_x chemistry, which includes the NO_2 -to- NO_x conversion factor f and the NO_2 lifetime τ . Figure 10 compares bottom-up and top-down emission estimates for the Belchatow and Jänschwalde power plants for the three approaches used for accounting for NO_x chemistry. The timeseries shows the estimates using the machine-learning (ML) model trained with GEOS-Chem simulation. The annual top-down estimates are shown using the default literature values for f (=1.32) and τ (=4 h) that were used outside Europe for the CSF estimates, the values from the ML model used inside Europe (Schooling et al. 2025), and values from plume-resolving chemistry simulations with the MicroHH model (Meier et al. 2024, Krol et al. 2024), which are only available for selected power plants.

The top-down estimates of annual NO_x emissions are quite similar using default and the ML model, because annual averages of NO_2 -to- NO_x conversion factor and NO_x lifetime from the model are quite consistent with the literature values. The NO_2 -to- NO_x conversion factors derived from MicroHH simulations are higher, slightly increasing the annual estimates. In addition, we used a lifetime of 2 h, which is the median found by Meier et al. (2024), when applying the CSF method to several cross sections downstream of the power plants, which allows for estimating the lifetime.

Overall, this limited analysis suggests that top-down estimates using the CSF method may underestimate NO_x emissions by approximately 20-50%.

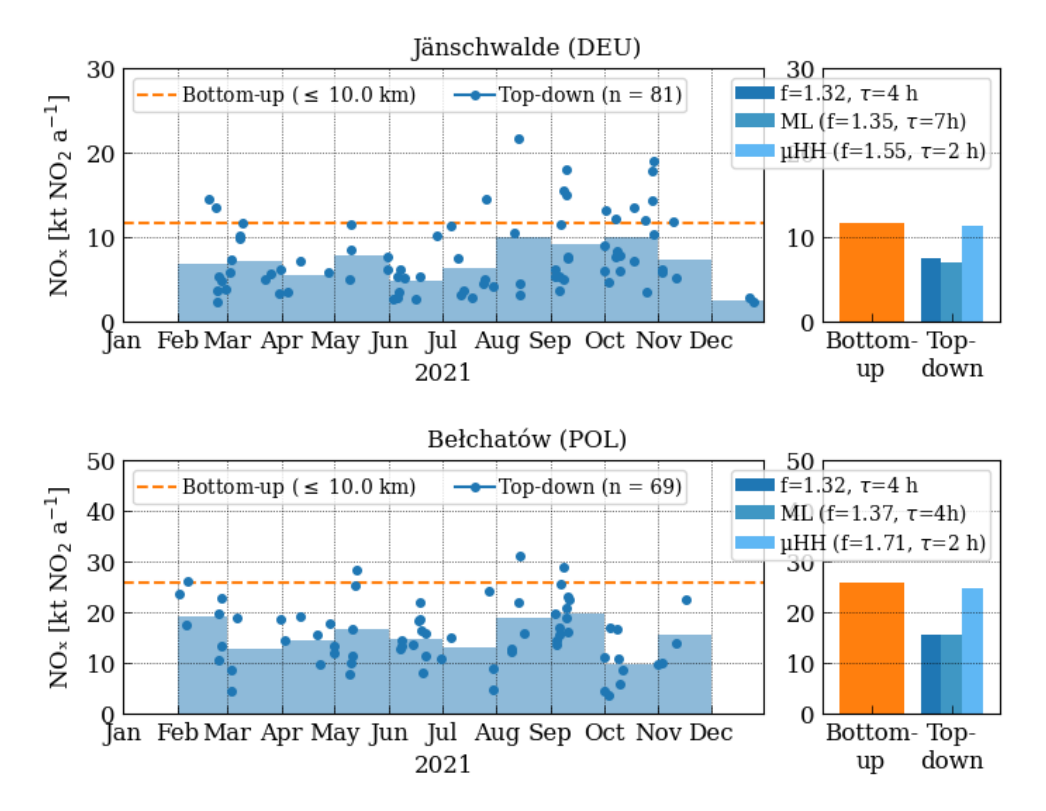


Figure 10 Comparison between bottom-up (orange) and top-down (blue colours) NO_x emission estimates for the Belchatow and Jänschwalde power plants. For the top-down estimates, three approaches were used for accounting for NO_x chemistry: default literature values for f (=1.32) and τ (=4 h), values from the Machine Learning (ML) model used inside Europe (Schooling et al. 2025), and values from plume-resolving chemistry simulations with the MicroHH model (Meier et al. 2024, Krol et al. 2024).

3.3 Consistency between annual CO emissions from iron and steel plants

3.3.1 Bottom-up emission estimates

For European plants, annual bottom-up emissions were mainly derived from the EU integrated Industrial Reporting Database, combining both the facility- and plant-level data into one location total. For the rest of the world, process-related CO emissions in I&S plants were computed for basic oxygen furnaces, electric arc furnaces and blast furnaces as well as for the production of coke combining I&S activity statistic with EF reported from the literature. National level emissions were spatially distributed across facilities considering information on their installed capacity for each operation. For more details on the description of the bottom-up estimation methodologies and sources of information considered, we refer to CORSO D1.2.

3.3.2 Top-down emission estimates

As part of CORSO WP2, Task 2.1 TNO investigated the use of TROPOMI CO to evaluate CO emissions plants from European iron and Steel (I&S) plants as reported under the European Pollutant Release and Transfer Register (E-PRTR) maintained by the EEA. The results are presented in CORSO WP2 deliverable D2.2 and published by Leguijt et al. (2025).

As part of that work, TNO and SRON first performed analytical inversions to estimate emissions from 21 individual plants using 2019 TROPOMI observations. Here, E-PRTR data was used for prior emissions, and WRF simulations were performed to replicate observed emission plumes. In this comparison between the E-PRTR and the inversion estimates a relatively good agreement was found but several plants showed a substantial deviation from the TROPOMI based estimates. As a second step TNO and SRON repeated the simulations for selected plants for more years which showed that over multiple years the consistency with the reporting improved (Leguijt et al., 2025). Since the WRF simulations are resource intensive, it was also tested if the CSF method as used in the African cities case study (Lequijt et al., 2023, also described in CORSO D2.2) would give reliable results for the I&S plants. Comparing the detailed WRF-based inversions with CSF estimates, agreement was found but it was shown that for I&S plants with a source strength below 100 kt CO per year the CSF results become less reliable (Leguijt et al. (2025). Leveraging the computationally lighter CSF method, in the present work we extended this method to I&S facilities outside of Europe. The main advantage is that since the method demands much less resources and time, it is possible to cover a much large selection of the global I&S plants.

The CSF method aims to calculate an emission rate *Q* associated with a single plume at a given location by calculating emission rates at various cross-sections of the plume (e.g. Krings et al., 2011, 2013; Varon et al., 2018, 2020; Sadavarte et al., 2021; Tian et al., 2022), often incorporating remote sensed observations. It does so by computing emission rates for many individual cross-sections across the plume, after which the average of these emission rates is taken as an emission rate for the source.

The CSF method is based on a mass balance equation on a closed surface:

$$Q = \oint U_{\perp} \Delta \Omega dA$$

Where Q is the emission rate in kg s⁻¹, U_{\perp} is the wind speed perpendicular to the closed surface. $\Delta\Omega$ (kg m⁻³) is the enhancement at the closed surface, and dA (m²) is a surface element. This equation is adapted to suit a column observation where the wind is not characterized as easily as on a closed surface, with a 2-dimensional derivation:

$$Q = \int U_{\perp}(x, y) \Delta \Omega(x, y) dy$$

Here, the x coordinate is along the wind direction, in the direction of the plume. The y coordinate is perpendicular to the direction of the wind, i.e. across the plume. $U_{\perp}(x, y)$ and

 $\Delta\Omega(x, y)$ are the wind perpendicular to the plume and the enhancement at the x and y coordinates, in m s⁻¹ and kg m⁻² respectively.

Since Q is independent of the distance to x, a multitude of cross-sections of the plume are calculated, after which they are averaged to produce an emission estimate \bar{Q} for the single plume:

$$\bar{Q} = \frac{1}{n} \times \sum_{i=1}^{n} \int U_{\perp}(x, y) \Delta \Omega(x, y) dy$$

To replace the wind speed perpendicular to the plume U_{\perp} with the estimated 'effective wind speed' U_{eff} , which is computed by:

$$U_{eff} = \beta_1 U_{10} + \beta_2$$

Where U_{10} is the wind speed at 10 meters altitude as provided in the ECMWF meteorological data in the TROPOMI CO product at time of overpass. The coefficients β_1 and β_2 (1.43 and - 0.92 respectively) are based on calibrations by Leguijt et al. (2023) using a simulated plumes method based on Varon et al. (2018).

In our application of the CSF method, we take all qualifiable overpasses for one location for an entire year, and use the yearly average as the final result, in accordance with the application of the method by Leguijt et al. (2025), to decrease uncertainties associated with single-overpass estimates.

Demostrating CSF application for a single location

Figure 11 exemplifies how the CSF method is applied to TROPOMI overpasses. Here, we see two overpasses over the ArcelorMittal Gent Iron & Steel plant in Gent, Belgium. These two overpasses are accepted by the algorithm to be included into the yearly estimate. Within one overpass and for one plume, multiple CO emission rate estimates are created in the form of transects of said plume, which are averaged into a single CO emission estimate. Here, we see that the emission rate in the left figure is 130 kt per year, while on the right, the emission rate is 70 kt per year. Additionally, we see that while some plumes are well characterized (top figure), other estimates could use improvement, as the bottom figure shows no clear plume pattern in the transects. Figure 12 illustrates the construction of the yearly estimate for this same location, where one yearly estimate (129 kt per year) is constructed from, in this location, 86 single overpass estimates.

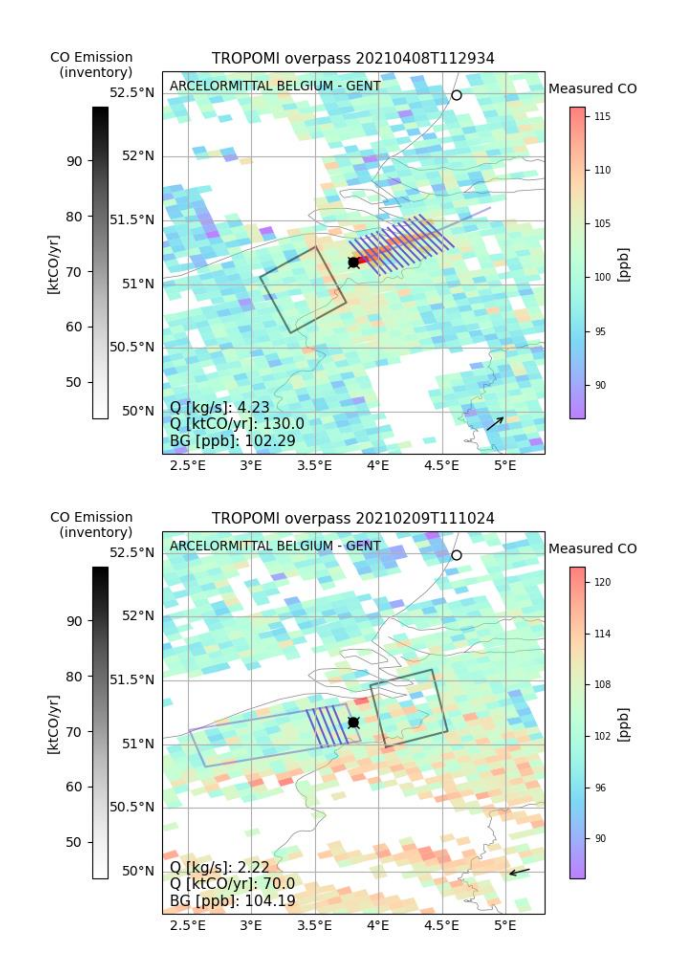


Figure 11 Two TROPOMI-based plumes of CO using the CSF method over the ArcelorMittal Gent Iron & Steel production facility in Gent, Belgium.

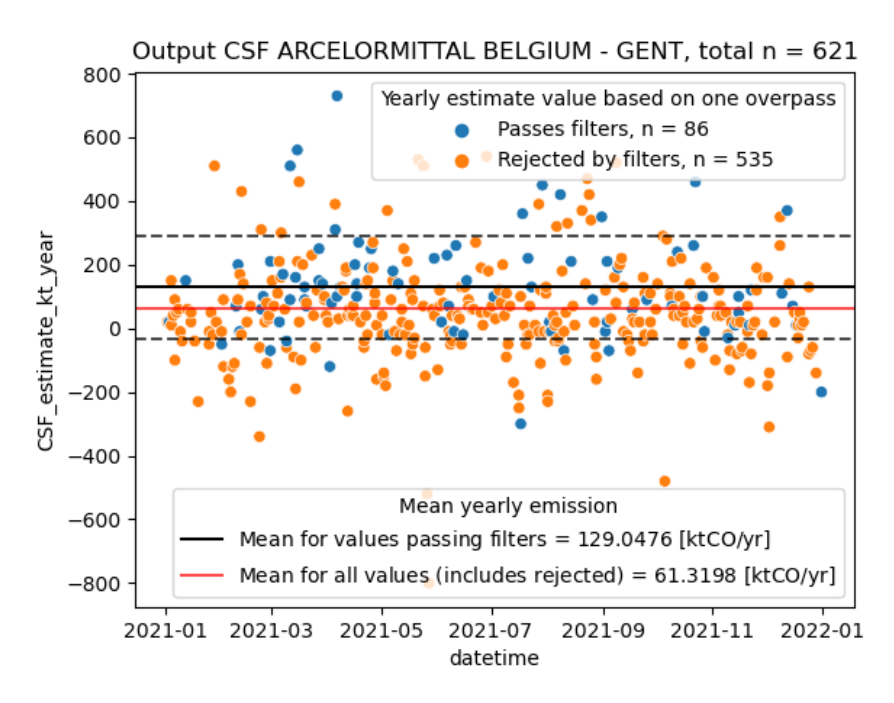


Figure 12 Overview of the passed and rejected CO TROPOMI-based estimates constructed using the CSF method, for the ArcelorMittal Gent I&S production in Gent, Belgium. Note that the average value, shown with the black line, is the only value considered certain enough to be

used in the context of this research. The dotted line represents the standard deviation as constructed from the passing estimates.

Comparison with previous CSF estimates

To increase the confidence in our current CSF application, we recreated CSF estimates already performed previously by Lequijt et al. (2025) and results that will be published by Leguijt et al. later this year (Table 1). It is important to underline that CSF estimates below 100 kt per year are not trusted as a valued estimate due to the sensitivity threshold of the method. The goal here, however, was replicability. We see that the CSF CO estimates constructed in this work shows good agreement with the CSF CO estimates constructed in previous work by Lequijt et al. for the locations 'Hüttenwerke Mannesman + ThyssenKrupp' (178 kt per year this work. 183 kt per year Leguijt et al.), 'POSCO Gwangyang' (487 kt per year this work, 472 kt per year Leguijt et al.) and 'Baotou' (1512 kt per year this work, 1430 kt per year Leguijt et al.). Moderate agreement is found in the 'Port Talbot Steelworks Tata Steel' (83 kt per year this work, 58 kt per year Leguijt et al.) and 'Arcelor Dunkerque' (122 kt per year this work, 170 kt per year Lequiit et al.) estimates. A larger discrepancy is found for 'ArcelorMittal Gent' (81 kt per year this work, 134 kt per year Lequijt et al.) requiring some additional investigation. Lastly, it is noticeable that for similar locations with similar results. CSF calculations from different overpasses are considered to be 'passing' for the CSF constructed in this work (Posco Gwangyang: 14 overpasses, Baotou: 89 overpasses) as opposed to previous work from Leguijt et al. (Posco Gwangyang: 36 overpasses and Baotou: 93 overpasses). Some differences between this work and Lequijt et al. can be attributed to differences in meteorology data used: while we use ECMWF, Lequijt et al. (2025) use GEOS meteorological input. Considering reasonable to good agreement between the estimates, we are confident that application of the CSF method with TROPOMI data can be done for the present validation work.

Table 1 Various estimates for plants that were included in previous work by Leguijt et al. (2025a, 2025b). Estimates include: i) CSF estimates from this work for 2019 and 2021, ii) CSF estimates from the work from Leguijt et al. (2025a, 2025b*) for 2019 and 2021, and iii) the CORSO bottom-up inventory, which targets 2021. *To be published later this year.

				2019		2021		
Location name	Country code (ISO3)	Latitude	Longitude	CSF Estimate ¹ , this work	CSF Estimate ¹ , Leguijt et al., 2025a	CORSO bottom- up inventory, this work	CSF Estimate ¹ , this work	CSF Estimate ¹ , Leguijt et al., 2025b
ArcelorMittal Gent	BEL	51.169929	3.804462	81 (75)	134 (-)	100	126 (86)	-
Hüttenwerke Mannesman + ThyssenKrupp	DEU	51.371279	6.72331	178 (103)	183 (-)	317	166 (114)	-
Posco Gwangyang	KOR	34.920086	127.74865	265 (6)	-	281	487 (14)	472 (36)
Baotou	CHN	40.647997	109.740898	1317 (97)	-	237	1512 (89)	1430 (93)
Port Talbot Steelworks Tata Steel	GBR	51.556	3.765	93 (47)	58 (-)	119	62 (108)	-
Arcelor Dunkerque	FRA	51.041274	2.292948	122 (42)	170 (-)	125	141 (58)	-

¹ number of estimates used given in brackets

3.3.3 Results of intercomparison

Since the largest point sources of CO are all Iron & Steel plants, they become the focus of this research. The locations of the top 66 CO emitting plants as per the CORSO bottom-up CO

inventory can be seen in Figure 13. A list of the country division can additionally be found in Table 2.

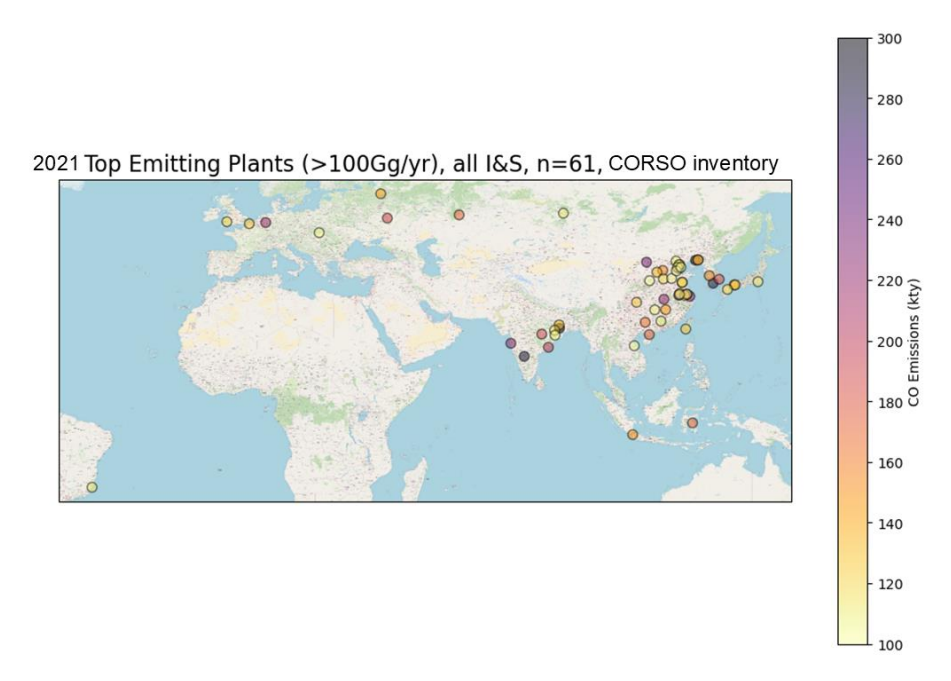


Figure 13 Top 66 CO emitting plants in kt per year for the year 2021, as reported in the CORSO bottom-up inventory. These are without exception Iron & Steel plants.

Table 2 Number of Iron & Steel plants per country in the top 66 global CO emitters as per the CORSO inventory. * South Korea.

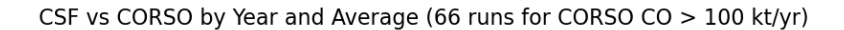
Country	ISO3 code	Number of I&S plants in top 66 CO emitters
China	CHN	37
Indonesia	IND	8
Russian Federation	RUS	4
Japan	JPN	4
The Republic of Korea*	KOR	3
Indonesia	IDN	2
Germany	DEU	1
France	FRA	1
Taiwan	TWN	1
The United Kingdom of Great Britain and Northern Ireland	GBR	1
Brazil	BRA	1
Slovakia	SVK	1
Vietnam	VNM	1
Belgium	BEL	1

We compared our yearly averaged top-down CSF results for these 66 plants for 2019, 2020 and 2021 with the 2021 CORSO bottom-up CO inventory estimates of these 66 plants.

As could already be seen in Table 1, the difference between a CSF-based estimate and a CORSO bottom-up estimate can differ substantially. To gain a basic understanding of the differences between the CSF and CORSO estimates, we include a simple comparison of the CSF top-down and CORSO bottom-up estimates with I&S facility level production data, as publicly available within the GEM online database. To do this, we select high CO emitting processes as proxy for CO emissions:

- When available, blast furnace iron production data
- If previous unavailable, total iron production data
- If previous unavailable, steel production data minus electric arc furnace steel production
- If previous unavailable, steel production data
- If none of this is available, we leave said plant out of the comparison

Figure 14 shows a comparison of a CSF constructed top-down emission rate estimate to the CORSO bottom-up emission estimate, for the top 66 CO emitters in the CORSO bottom-up inventory (when successful for both methods). For the CSF method, his is done for the years 2019, 2020 and 2021, as well as an average of these three years. Note that the CORSO inventory is made for the year 2021, but as the CSF depends on available overpasses with high-quality data (no clouds, etc) the CSF estimate becomes more robust when averaged over multiple years. We see that the CSF estimates show a much higher variation in estimates than does the CORSO emission inventory, for all years. We also see that there are many CSF estimates in agreement with the CORSO bottom-up inventory. The individual location values seem somewhat comparable across the different years.



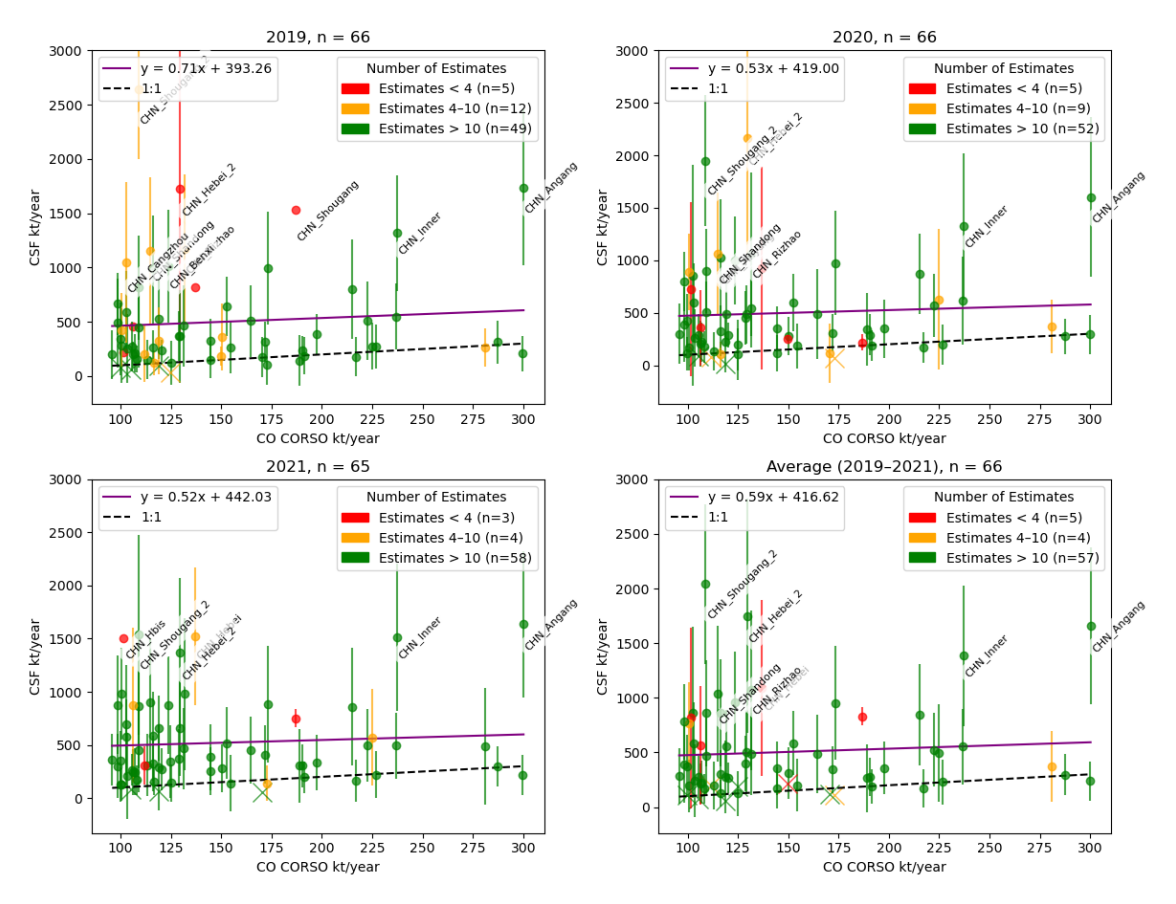


Figure 14 Average values for CO estimates using the CSF method with TROPOMI for the top 66 locations of the CORSO bottom-up inventory, in kilotonnes per year, for the years 2019 (top left), 2020 (top right), 2021 (bottom left) and the 2019-2021 average (bottom right). Linear regression and 1:1 line is included in all figures. Locations are colour coded for the amount of yearly estimates used to create the yearly average value. The 'x' indicates a location with a CSF estimate of < 100 kt per year, which is hence not an estimate that adheres to our criteria of valid estimates.

Figure 15 shows the CSF:CORSO ratio on a country level, for the year 2021. There is a clear difference between China and the rest of the world: while the ratio is 5.16 for China, most other countries' ratios range around 1.13-2.5, with Brazil and Taiwan both having a higher ratio of 2.74, but in both cases the sample is limited to one plant only. We note that the Slovakian (SVK) I&S plant, the British (GBR) I&S plant and one Chinese (CHN) I&S plant have values below 100 kt a year threshold value and thus that their contribution to the ratio is not seen as a valid result. For the sake of the disclosure of this analysis, they are kept included in this figure.

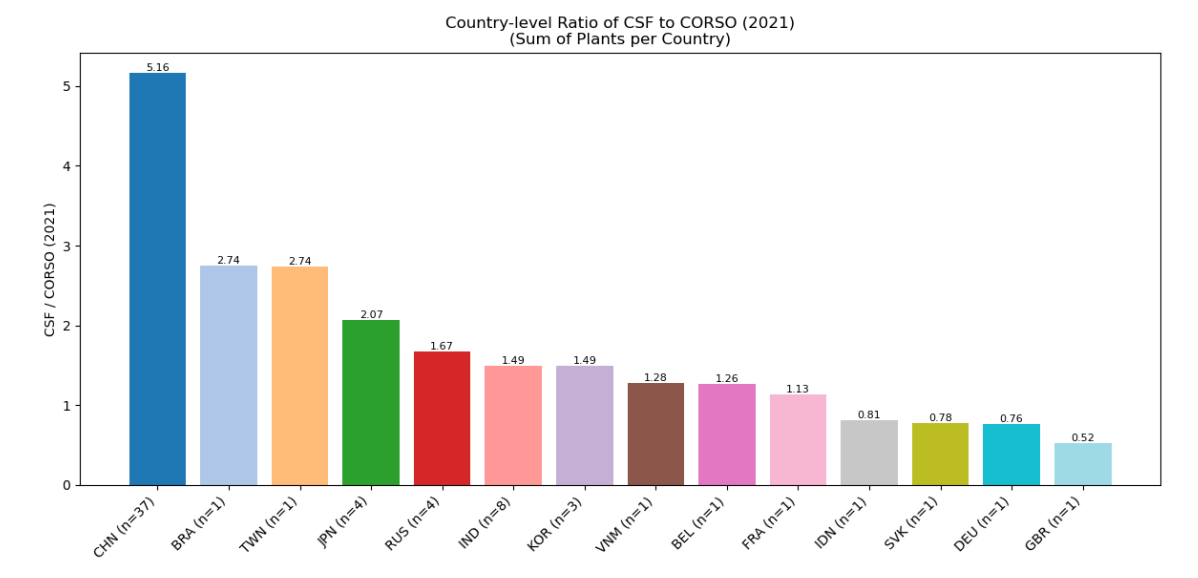


Figure 15 Ratio of CSF CO values to CORSO CO values, averaged for the different countries included in the top 66 CO emitters in the CORSO bottom-up inventory, as used for the creation of CSF TROPOMI estimates.

To inspect the noticeable discrepancy between the Chinese ratio of the CSF top-down CO estimate to the CORSO bottom-up CO estimate, the estimates were compared with available I&S production data, as is seen in Figure 16. In this figure, a comparison is shown with an emission proxy of the I&S production on the x axis. These comparisons are plotted for the year 2019, 2020 and 2021. This exercise is shown three times: once for all locations, once for China separately, and once for all countries except China. It becomes clear that outside of China, the CSF top-down estimates and CORSO bottom-up estimates are in considerably reasonable agreement, albeit higher.

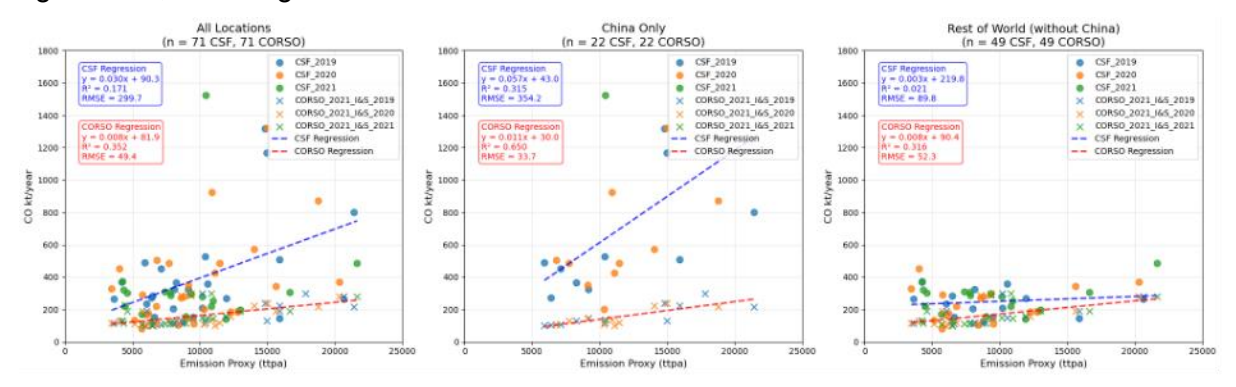


Figure 16 The CSF top-down CO estimates and CORSO bottom-up CO estimates (both in kt per year), plotted against an emission proxy of the I&S production (in ttpa = Thousand Tonnes Per Annum), for the year 2019, 2020 and 2021. The I&S production data was retrieved from the Global Energy Monitor (GEM) database. Left panel: all locations where production data was available. Middle panel: only Chinese locations, where production data was available. Right panel: all countries but China, for locations where production data was available.

As can be seen in Table 3, the emissions proxy values based on production data show a slightly higher mean proxy value for China only (11 571) as compared to other countries (8 933) for the available data within 2019-2020-2021. Meanwhile, the mean CSF for 2019-2020-2021 for China only is much higher (1659) than is the mean value in other countries (399). The CORSO 2021 CO inventory data shows a mean value of 154 for China only and a mean value of 168 for all countries but China, showing a contradictory trend. It must be noted that the CORSO value is partially constructed with the GEMS data used to create this emission proxy, so a trend between the two are to be expected.

Table 3: The averaged 2019-2020-2021 CSF values, emission proxy values based on GEMS I&S production data, and CORSO 2021 inventory values for plants where I&S production data was available, for A) Plants in all countries included in this study, B) Plants in all countries excluding China, C) Plants in China only. Note that each plant may or may not have production data in different years (2019-2020-2021).

A) Included I&S plants in all countries (n = 32)						
	CSF 2019-2020- 2021 (kt/year)	Emission proxy 2019-2020-2021 (ttpa)	CORSO 2021 (kt/year)			
min	129	3 807	98			
max	1 659	20 861	300			
mean	441	10 088	162			

B) Included I&S plants in all countries excluding China (n=18)					
	CSF 2019-2020- 2021 (kt/year)	Emission proxy 2019-2020-2021 (ttpa)	CORSO 2021 (kt/year)		
min	129	3 807	101		
max	399	20 861	300		
mean	245	8 933	168		

C) Included I&S plants in China only (n=14)						
	CSF 2019-2020- 2021 (kt/year)	Emission proxy 2019-2020-2021 (ttpa)	CORSO 2021 (kt/year)			
min	215	5 900	98			
max	1 659	20 082	300			
mean	694	11 571	154			

We have started to investigate several issues to interpret the difference in the ratio of CSF top-down CO estimates to CORSO bottom-up CO estimates. To improve the robustness of CSF estimates, it will prove useful to implement stricter filtering to the top-down algorithm based on a critical assessment of the individual overpass emission estimate result. Utilizing TROPOMI data on locations near large water surfaces imposes challenges, as the observations are often lacking over these waters. This causes difficulties in estimating background concentrations, which is a prerequisite to estimate emissions with the CSF method. Additionally, when plants are situated near mountainous areas, the elevation can cause the flow of pollutants to move in different directions than they would over flat areas, possibly causing some challenges to the CSF estimate. No evidence of this effect was found

CORSO

in a visual assessment of the results so far, but as a common issue, this needs to be kept as a possible point of attention. Another issue for satellite observations is the heterogeneity in clouds, where different characteristics within clouds can have a variety of effects on the satellite observations. We will continue assessing our CSF method taking these effects into account and improve our method where necessary. A possible outcome can also be that the method could only be applied to locations in land-inward regions, for example

As a part of this deliverable, locations were arranged to include nearby locations and urban areas, thereby pinpointing possible co-emitting sources near each other which could lead to plume mixing. While strongly underling the necessity of taking this effect into account, this has not yet been considered for the creation of CSF estimates in this deliverable, with one exception for the comparison with an estimate previously composed by Leguijt et al. (2025) in Germany. It is important to take this effect into account, because otherwise, there is a current risk of measuring the total emission of neighbouring plants' twice as individual measurements.

Lastly, to better be able to understand the differences between countries, we aim to start using the top 120 CO emitters from the CORSO bottom-up CO inventory, rather than the top 66. This is only possible because we do see that many CSF estimates rank higher than 100 kt per year, which was stated to be the minimum CSF yearly estimate. Considering more targeted point sources will include a larger variety of plants across various country, thereby increasing the breadth of our cross-country analysis.

More investigation on the potential causes of the high CSF CO estimate of the Chinese plants compared to bottom-up estimates, as well as the relative difference in the height of these estimates compared to plants in other parts of the world, remains necessary.

3.4 Daily variations of NO_x emissions

3.4.1 Bottom-up emission estimates

Day-of-the-year NO_x emissions estimates for the year 2021 were collected for the top 10 NO_x emitter coal-fired power plants in the USA. The data was derived from the <u>EPA Clean Air Markets Program Data</u> and is based on the continuous emission monitoring systems (CEMS) installed in each power plant.

3.4.2 Top-down emission estimates

Top-down estimates were derived using the CSF method described in Section 3.2.2. The CSF method provides individual emission estimates at satellite overpass with an accuracy of about 30%. Enough overpass should be sufficient to resolve some day-to-day variability.

3.4.3 Results of the intercomparison

Figure 17 compares bottom-up and top-down NO_x emissions for the 10 selected U.S. power plants. Annual emissions agree quite well with a mean bias of -0.5 kt (-5%) and a scatter of 2.5 kt (30%). The mean bias is larger (-12%) and scatter is smaller (19%) when excluding Hunter power station, where the plume often overlaps with the nearby Huntington power plant (6 kt). We expect that we underestimate top-down estimates by about 20-50% due to using default values for NO_x chemistry (see Section 3.2.3 for more details).

The time series for selected power plants shows that satellite-based estimates are able to identify the seasonal cycle quite well. For example, Labadie power plant has very constant emissions throughout the year, which is also shown in the top-down estimates. In contrast, Miami Fort power plant has high emissions in winter and low emissions in summer. This is also clearly observed by the satellite instrument. The Intermountain power plant shows very strong temporal variability, which is partly covered by the satellite instrument. However, comparing daily means with TROPOMI overpass values becomes challenging, as hourly values may vary a lot during the day.

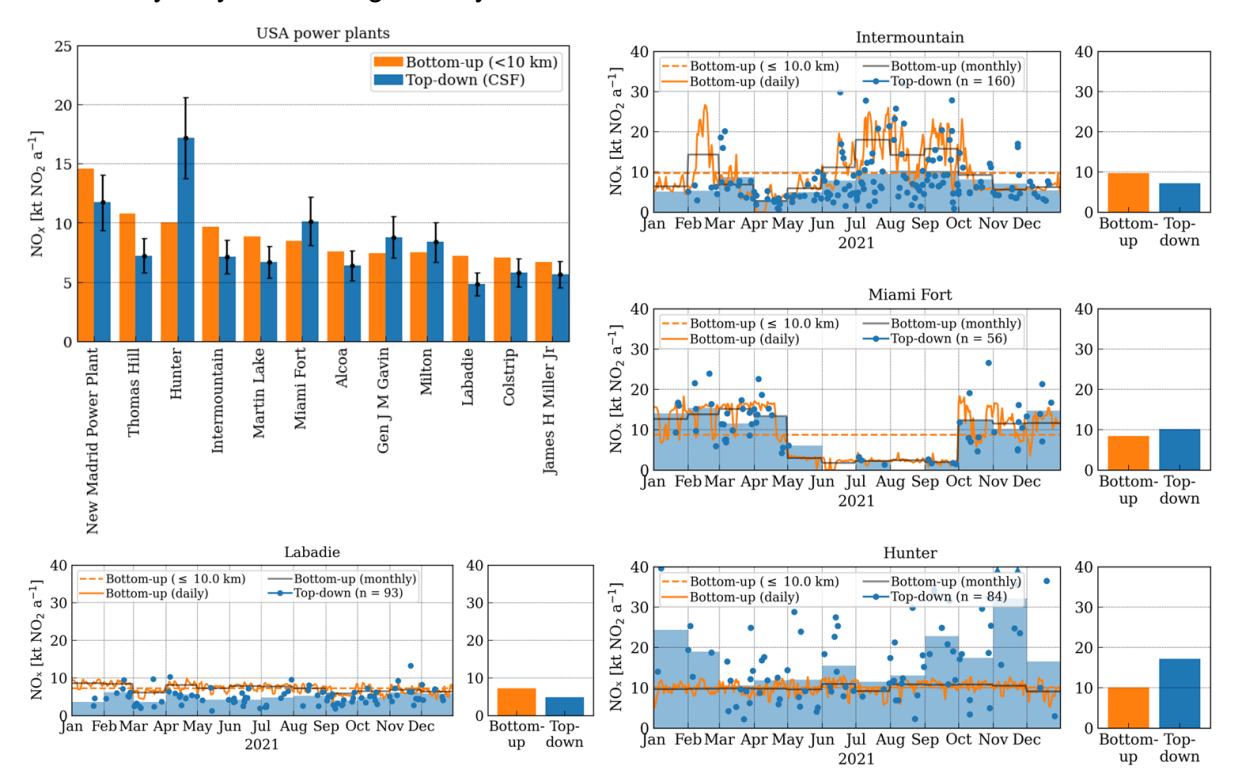


Figure 17 Comparison of daily bottom-up and top-down NO_x emission estimates for USA power plants for 2021.

4 Revised version of the CORSO point source catalogue

The discrepancies identified and described in sections 3.1 and 3.2 translated in a series of updates and improvements of the original CORSO point source database developed as part of T1.2. We refer to this new version of the catalogue as the CORSO point source database version 2. The following list provides a summary of the improvements performed:

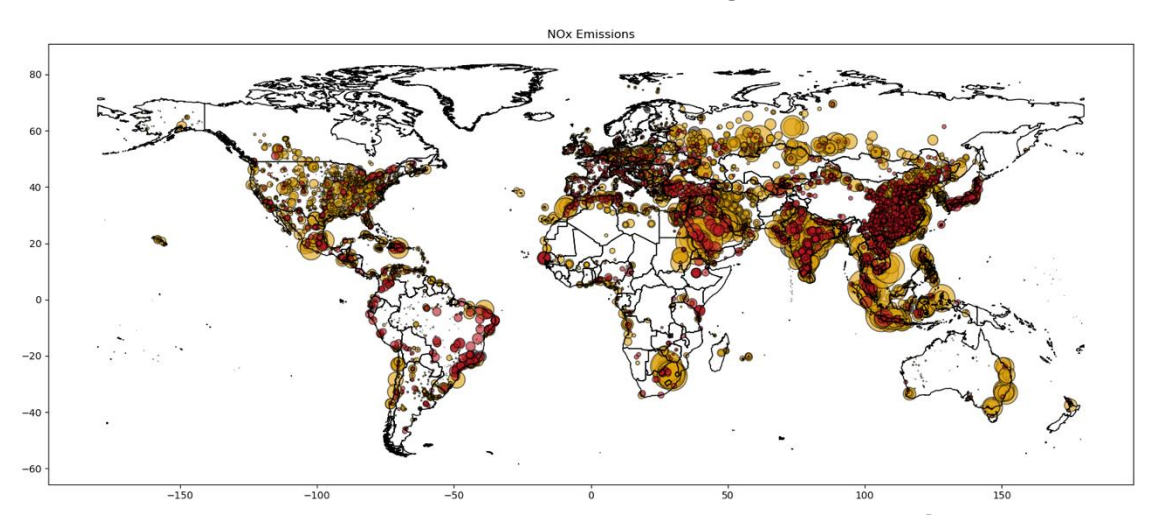
- Correction of location of plants: Geographical locations for a total of 41 plants were corrected. These corrections were made in Lebanon, Brazil, Venezuela, Spain, Africa, Saudi Arabia, Pakistan, Iraq and Bangladesh.
- Addition of missing plants: A total of 8 unlisted facilities were added to the revised version of the bottom-up catalogue, including three large point sources, namely the Kosovo A and B lignite-fired power stations and the Secunda synthetic fuel plant, located in South Africa. For the other cases (5 out of 8), the added plants were small and isolated power plants with installed capacities below 50 MW.
- Update of country- and fuel-dependent emission ratios
 - Indonesia, Malaysia & Philippines: new NO_x:CO₂ and SO_x:CO₂ emission ratios for coal-fired power plants based on Triani et al. (2024).
 - <u>Lebanon:</u> new NO_x:CO₂ emission ratios for oil-fired power plants based on MoE/UNDP/GEF (2021).
 - Rest of the world (excluding EU27+UK and USA): Moving from country and fuel-dependent NO_x:CO₂, SO_x:CO₂ and CO:CO₂ emission ratios computed with CEDS v2024_07_08 (Hoesly et al., 2024) to a new set of ratios computed using CEDS v2025_03_18 (Hoesly et al., 2024)
- Review split of dual fuel power plants
 - CORSO version 1: For dual-fuel plants using both natural gas and oil, we: i) duplicated them, ii) assigned one single fuel to each duplicate (i.e., oil or natural gas) and iii) split the total installed capacity according to the oil versus natural gas consumption reported by IEA in the country where the plant is located.
 - CORSO version 2: assumed dual fuel plants only consume their primary fuel as reported by the Global Energy Monitor (GEM) Global Oil and Gas Plant Tracker database. For Kuwait, we consider the plant-level fuel split information reported by Alkheder and Almusalam (2022).
- Correction of bug associated to the filtering of "operating" units: In CORSO version 1, GEM units starting operation after 2021 were kept by mistake. The bug was corrected in CORSO version 2, which implied the removal of 163 units. The most affected countries were China (removal of 15 units), Iran (removal of 14 units) and India (removal of 8 units). National emissions where remapped to the existing units.
- Review description (location and installed capacity) of oil-fired power plants: The locations and installed capacity of oil-fired power plants in Saudi Arabia, Iraq, Pakistan, Kuwait and Lebanon were revised making use of the GEM's Global Oil and Gas Plant Tracker, replacing the information reported by the IndustryAbout and WRI power plant databases, which are not maintained any more.

4.1 Impact on the bottom-up emission estimates

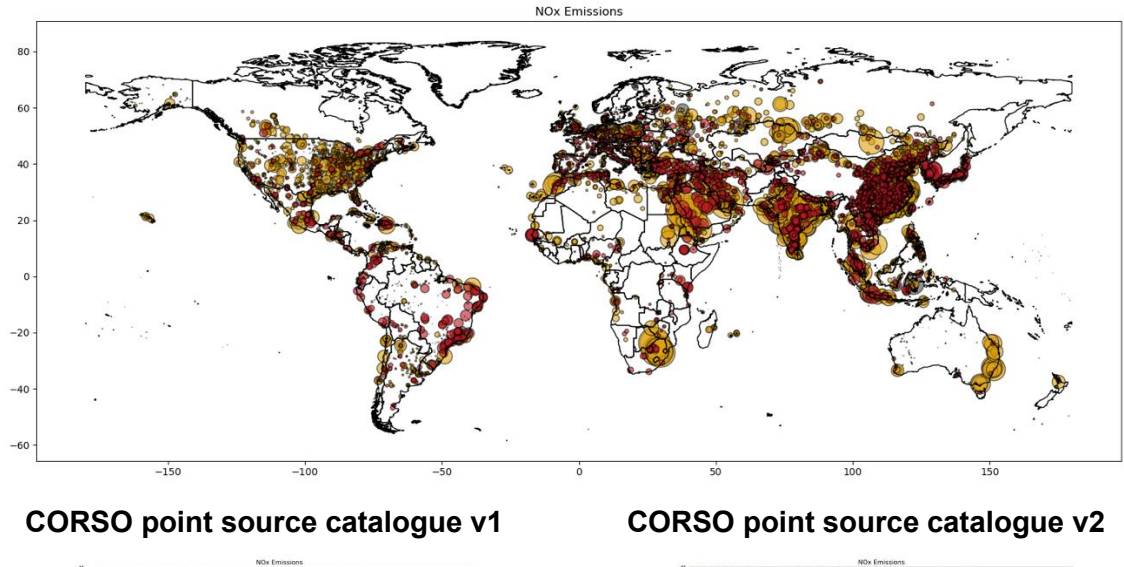
Figure 18 shows the plant-level annual NO_x emissions as reported by the versions 1 and 2 of the CORSO bottom-up point source database, with a zoom over the Middle East, were the impacts of the updates performed can be clearly identified. Results are distinguished by industry type (power, cement and I&S). It is observed that the emission intensity reported by power plants in Southeast Asia (Philippines, Malaysia, Indonesia) is much lower in version 2

of the catalogue due to the review of the emission ratios. Several hotspots in Saudia Arabia are also reduced in version 2, especially in the East coast. A few new power plants are observed in Northern Africa as a result of the NO_x hotspot location validation work (Section 3.1). Results for CO_2 are not reported because changes in emissions between the two versions of the datasets are negligible (-0.14%).

CORSO point source catalogue v1



CORSO point source catalogue v2



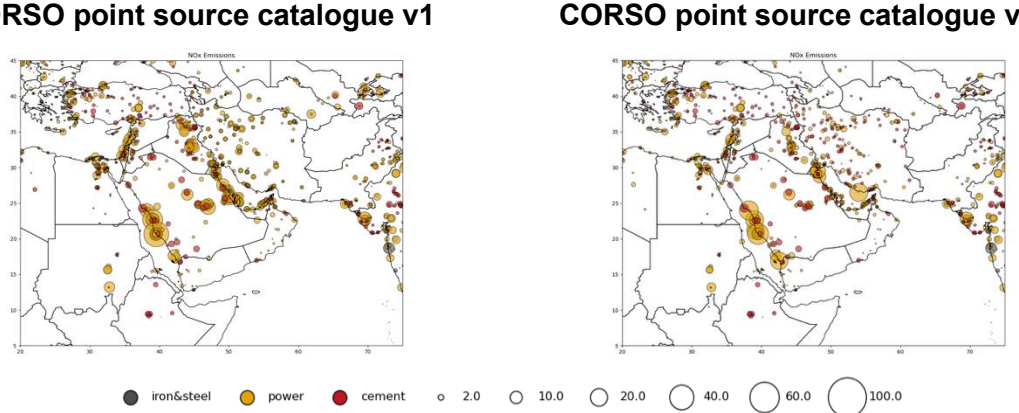


Figure 18 Plant-level annual NO_x emissions (kt/year) reported by the CORSO global point source database versions 1 and 2, with zooms over the Middle East

Figure 19 shows a comparison between NO_x country-level emissions as reported by the versions 1 and 2 of the CORSO bottom-up point source database. Results include only those countries in which total emissions changed between the two versions of the catalogue. Large reductions (more than -50%) are reported in several countries such as Indonesia (IDN), Malaysia (MYS), Russia (RUS), Bangladesh (BGD) or the United Arab Emirates (ARE), which are mainly driven by the updates of the NO_x : CO_2 emission ratios described at the beginning of Section 4. At the global scale, the updates performed in version 2 of the catalogue translated into a -19.35% decrease of total NO_x emissions when compared to version 1.

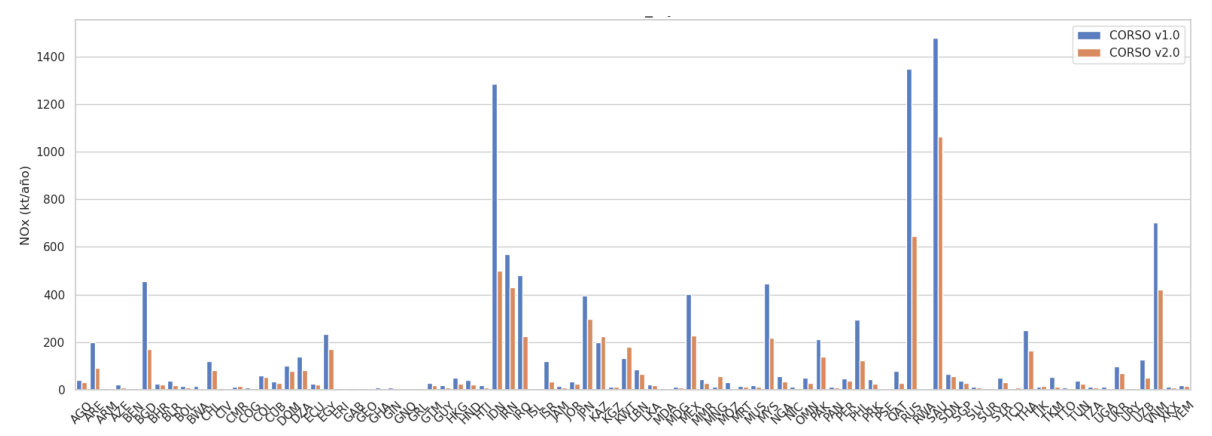


Figure 19 Comparison between country-level NO_x annual emissions [kt/year] estimated by the CORSO point source database versions 1 and 2.

4.2 Impact on the consistency with top-down emission results

Figure 20 and Figure 21 present the results of the comparison between plant-level annual NO_x emissions estimated by the CORSO bottom-up catalogue version 1 (blue) and version 2 (green) and derived from TROPOMI (orange) using the divergence method for selected countries, including South Africa, Saudi Arabia, Indonesia, Bangladesh and Lebanon. Grey bars represent the bottom-up emissions from other CORSO point sources located within the integration radius considered in the top-down estimates. Black dots highlight those power plants that are within 10 km of a city classified as rank 1 or rank 2 by the <u>ESRI World urban areas</u>.

The updates performed to the bottom-up catalogue and listed at the beginning of Section 4 have generally translated into a much better agreement with the top-down estimates. Examples of that are the Kusile power plant in South Africa, which installed capacity was reviewed in version 2 of the catalogue, the Qurayyah and Ras Al-Kair and Riyadh 12 power plants in Saudi Arabia, which are now treated as natural gas power plants, or most of the Indonesian power plants, which NO_x:CO₂ emission ratio was reviewed. Despite the general improvements, large inconsistencies are still reported for some plants. Examples of these are the Gazipur oil-fired power plant in Bangladesh and the Zouk 1 power plant in Lebanon, where the bottom-up emissions are approximately 5 times lower than the ones reported by the topdown estimates. For the first case (Gazipur, Bangladesh) we hypothesise that the discrepancy is mainly related to a limitation with the approach considered for the allocation of the estimated bottom-up emissions across power plants. As previously explained, for non-European countries power plant emissions are first estimated at the national level and then distributed across plants considering their installed capacity. This method does not consider the capacity factors of the plants (i.e., ratio of actual electrical energy output to the theoretical maximum electrical energy output) and therefore assumes that all of them are running at the same capacity. Nevertheless, important differences can exist between plants, especially in the case of oil-fired power plants, as some of them are typically used as peaking power plants and run only when there is a high demand. For the case of Bangladesh, the annual reports produced

by the <u>Bangladesh Power Development Board</u> indicate large variations in the capacity factor across oil-fired plants, indicating that our method could potentially be over/under-allocating emissions in some of them. For the second case (Zouk 1, Lebanon), we hypothesise that the top-down estimates include not only the emissions from the power plant, but also from Beirut, which is located less than 10 km away from the facility, and industrial and urban plumes observed by TROPOMI cannot be distinguished in the divergence method (Figure 22).

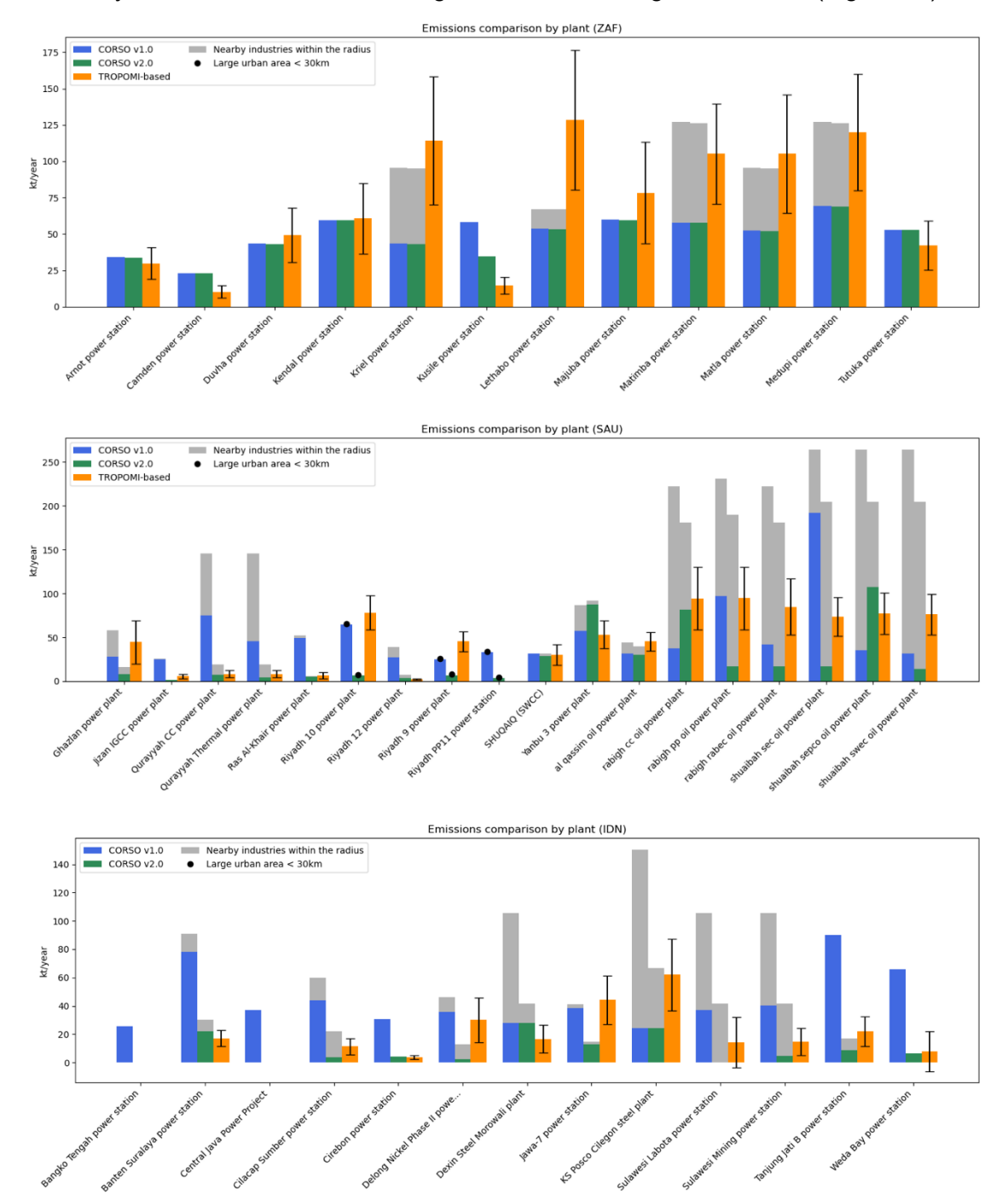


Figure 20 Comparison between plant-level annual NO_x emissions estimated by the CORSO bottom-up catalogue versions 1 (blue) and 2 (green) and derived from TROPOMI using the divergence method (orange) for selected countries, including: South Africa, Saudi Arabia, and Indonesia.

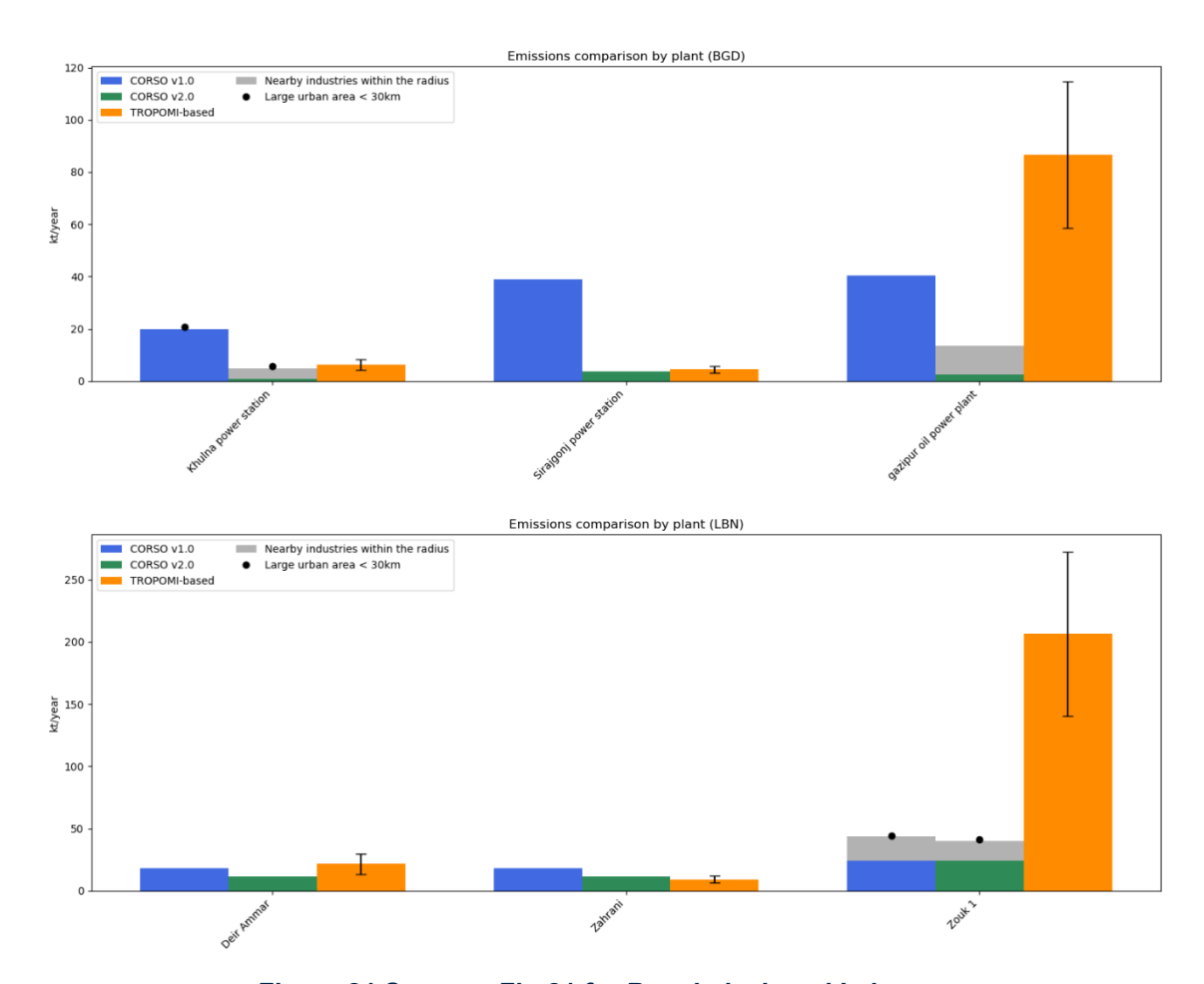


Figure 21 Same as Fig.21 for Bangladesh and Lebanon

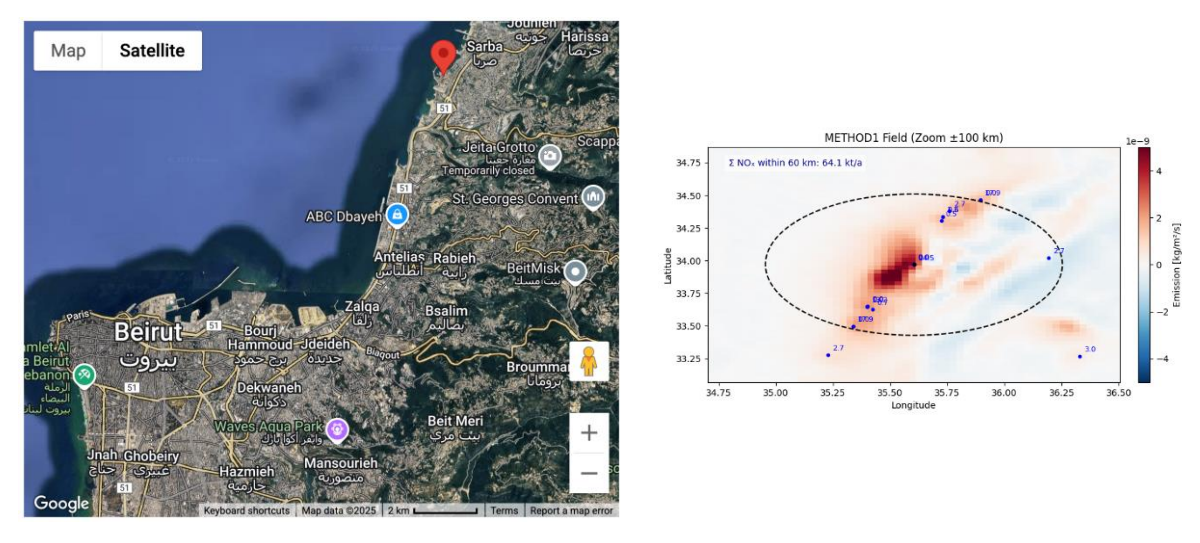


Figure 22 Location of the Zouk oil-fired power plant in Beirut, Lebanon (left) and integration radius considered to derive TROPOMI-based NO_x emissions for this power plant

Figure 23 presents country-level ratios of the NO_x emission estimates reported by the CORSO bottom-up point source catalogue (version 1 in blue; version 2 in orange) to the estimates derived from the TROPOMI-based divergence method. The ratios per country are estimated as the median of the ratios computed per individual facility. Only countries for which at least three facilities are available are included in the plot. The updates introduced in version 2 of the CORSO bottom-up point source catalogue have led to a much better consistency with the top-down estimates, the ratios being close to 1 in most of the countries.

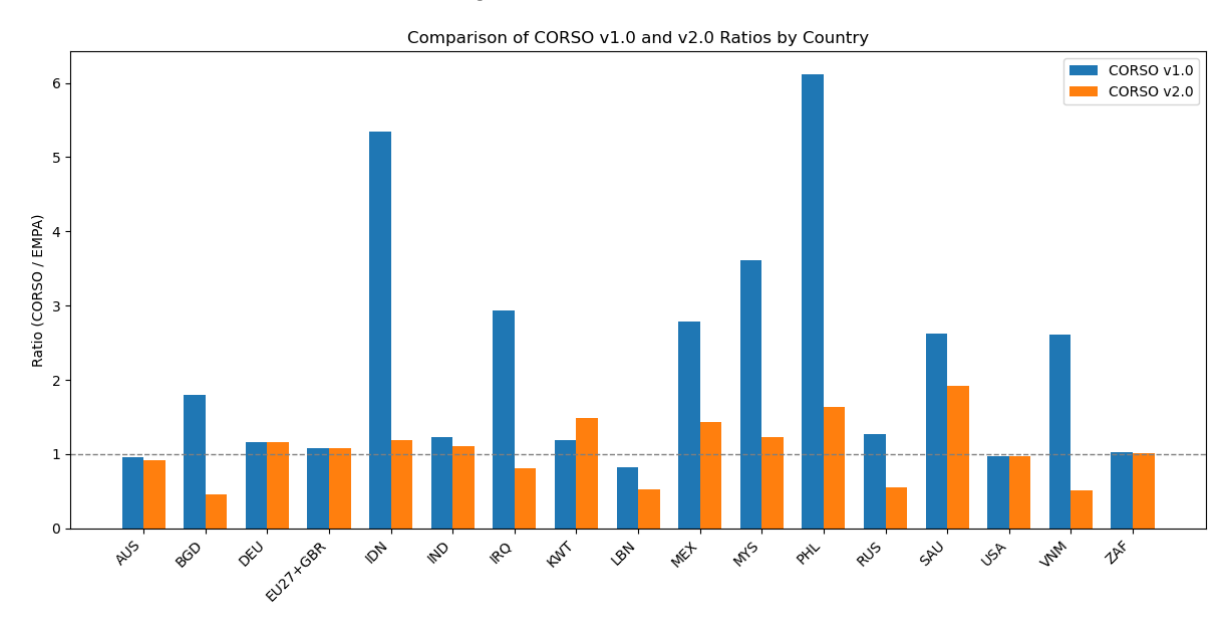


Figure 23 Ratios between the NO_x emission estimates reported by the CORSO bottom-up point source catalogue (version 1 in blue; version 2 in orange) and the TROPOMI-based divergence method per individual country and the EU27 + UK.

4.3 CORSO point source catalogue version 2

The new version of the CORSO bottom-up point source catalogue can be downloaded from the following public FTP:

Server: es-ftp.bsc.esUsername: mguevara

Password: p5SEEZDU/i8niLLG

- Port: 8021

And the files are stored in the following path: mguevara/ corso/corso ps v20

The final database is composed of the same files and information fields as its predecessor, as described in D1.2. Note that no changes were performed to the temporal and vertical profiles provided with the point source catalogue. A description of the methodologies and datasets considered to develop these profiles is reported in D1.2.

The top-down emission estimates described in this deliverable are reported as part of D2.2.

5 Conclusions and recommendations for future improvements

This document presents the results derived from intercomparing the global bottom-up point source catalogue developed as part of CORSO T1.2 against a collection of TROPOMI satellite-based (top-down) emission products estimated in CORSO T2.1, including lists of global NO_2 hot spots, NO_x and CO annual estimates from individual industrial plumes and plant-level daily variations of NO_x emissions. The rerefence year of the intercomparison exercise is 2021 for all the cases. For a detailed description of the estimation methods considered to compute the bottom-up and top-down emission products, we refer to CORSO deliverables D1.2 for the bottom-up point source catalogue and D2.1, D2.2 and D2.3 for the top-down emission estimates.

The comparison between top-down and bottom-up industrial hotspot locations resulted in the identification of wrongly allocated plants in the bottom-up catalogue as well as missing power plants, including both isolated plants with installed capacities below 50 MW but also large coal-fired power plants located in Kosovo and South Africa. These findings will be reported to the <u>Global Energy Monitor trackers</u> (GEM) initiative, so that our findings can be considered in future releases of their point source databases. A manual inspection revealed other strong emission sources observed by TROPOMI and that are currently not included in the bottom-up catalogue, mainly refineries and mining activities (e.g., copper smelters, cobalt refineries).

The consistency between bottom-up and top-down NO_x plant-level emission estimates was performed across 173 individual power plants and 20 European I&S plants. A good agreement between the bottom-up and TROPOMI-based estimates was reported for EU27+UK and USA power plants. The consistency observed in these two regions provides confidence in the top-down results, as the bottom-up emissions are based on the officially data reported by the EU integrated Industrial Reporting Database and the EPA eGRID database, which for large power plants typically rely on emission monitored data. Results also indicate a good match between bottom-up and top-down estimates in countries dominated by coal-fired power plants, such as South Africa, India or Australia, the bottom-up estimates from each plant being generally within the range of uncertainty provided by the top-down results. For some countries such as Saudi Arabia and Indonesia, large discrepancies between the emission estimates are observed across most of the power plants, the bottom-up catalogue generally reporting much larger emissions than the top-down estimates.

Concerning the validation of NO_x emissions from I&S plants, we found that top-down estimates significantly exceed bottom-up reports. The discrepancy likely arises because I&S plants are often situated in industrial zones, where we expect additional emissions from smaller but numerous sources from other sectors as well as from residential/commercial heating and traffic emission sources, which are not included in the CORSO bottom-up point source catalogue. Due to the relatively low emissions from the I&S plants, these surrounding sources may contribute more significantly than in regions dominated by major emitters, such as those identified as part of the Top NO_x emitting power plants.

Regarding the intercomparison between bottom-up and top-down CO annual emissions for I&S plants, our analysis showed that for Europe with an industrial reporting directive, the top-down estimates and bottom-up emissions agree relatively well. However, when we look at the global scale, the top-down CO estimates are generally higher than the CORSO bottom-up CO estimates. Most of the I&S plants analysed (37 of 66) are in China, and these plants show strikingly high CSF CO estimates compared to the bottom-up CORSO CO estimates. For all other countries, while generally the CSF top-down CO estimates were higher than the CORSO bottom-up CO estimates, the differences between the two were not nearly as vast as the differences for China. Investigating the production data did not provide a reasonable assessment as to where these differences come from. Further research to investigate the observed discrepancies is needed.

Day-of-the-year bottom-up and top-down NO_x emissions for 10 selected U.S. power plants were compared. Annual emissions agreed quite well, and the time series for selected power plants showed that satellite-based estimates are able to identify the seasonal cycle quite well. However, comparing daily means with TROPOMI overpass values becomes challenging, as it is not known during which time of the day emissions occurred.

The validation process performed in this work consisted on an iterative process, in which firstly bottom-up estimates were compared against the satellite-based emissions to flag inconsistencies, then paths for improvements and/or correction of bugs were identified based on these inconsistencies and, when possible, implemented in the bottom-up estimates, and finally a new round of intercomparisons were performed to assess the impact on the consistency of the results an progress towards a better convergence.

As a result of this validation process, we enhanced the quantification of emissions and addressed misallocations and the inclusion of missing facilities in the bottom-up CORSO emission catalogue, reducing the gap with the satellite-based estimates and demonstrating the added value of integrating bottom-up and top-down emission estimation methodologies. A revised version of the bottom-up point source catalogue was produced and is reported as part of the present deliverable. This new version of the catalogue, to which we refer as CORSO point source database version 2, replaces the previous one produced as part of D1.2. The improvements performed were as follows:

- Correction of the geographical location of plants
- Addition of missing plants
- Update of country- and fuel-dependent NO_x:CO₂ and SO_x:CO₂ emission ratios
- Review split of dual fuel power plants
- Correction of bug associated to the filtering of "operating" units:
- Review geographical location and installed capacity of oil-fired power plants in selected countries

A series of recommendations for future improvements of the prior bottom-up emission catalogue and the top-down emission estimation methods were also identified.

Recommendations related to bottom-up methodologies:

- Inclusion of additional large emitting industrial sources, namely refineries and industrial plants related to mining activities (e.g., copper smelters and cobalt refineries). As reported by the TROPOMI-based NO₂ industrial hotspot locations, these types of facilities can be very relevant in African (Zambia, Democratic Republic of the Congo) and Latin American countries (e.g., Chile, Peru).
- Improvement of the metadata considered for the power plants. Detailed information on the capacity factor and after treatment devices included in specific plants can be critical for a correct estimation of co-emitted species (NO_x), especially in countries with a large number of peaking power plants and where technologies vary significantly between facilities. Although this information is not always available and compiling it may be very challenging, dedicated investigations could be performed in those countries where the discrepancies between bottom-up and top-down results are large.
- Improvement of the emission ratios and emission factors considered for power plants and I&S plants, respectively. For power plants, the use of country- and fuel-dependent emission ratios derived from CEDS allows to reflect the influence of national legislation and degree of penetration of aftertreatment devices. However, the current validation works highlighted that for some countries (e.g., Lebanon, Philippines) the emission information reported by CEDS was not correctly reflecting these factors, and independent national emission information had to be considered to reduce the discrepancies with top-down estimates.

CORSO

• Inclusion of a unique identifier for each plant in the CORSO point source database that does not change between versions. This identifier may help tracking the changes performed between versions of the catalogue, as names of power plants may slightly change between versions or contain characters that difficult their match.

Recommendations related to top-down methodologies:

- A better understanding of uncertainties of top-down methods to better quantify the systematic uncertainty especially due to NO_x chemistry at plume scale, which will be necessary for assimilation of top-down estimates in the inversion system.
- A satellite image of an emission plume might not yield an estimate for various reasons:
 The image is partly or fully cloudy covering the plume, emission estimate fails due to complex situations such as low wind speed or overlapping plumes. The emission strength is below the detection limit of the instrument, which depends on wind speed and other parameters, or the source is not emitted at overpass time. A method needs to be developed to flag estimates that are below the detection limit or failed estimate.
- The analysis focused on isolated point source without other nearby sources. However, the majority of point sources are located in source clusters, where the emission plumes of multiple sources are overlapping. To develop a hot spot emission quantification system, it will be necessary to advance methods that can handle point source clusters.
- Several steps will be taken to assess where the CSF method considered for the estimation of CO top-down emission might need improvement to be able to strongly assess I&S plants across the world. These include to sensitively align our CSF method with the challenges that satellite data imposes, such as challenges regarding water bodies, effects of clouds, and elevation effects. Additionally, the summation of emissions of nearby plants will be imposed. Lastly, the analysis will be extended to the top 120 plants in the CORSO inventory, to get a more comprehensive overview of the plants that yield us results above the 100 kt per year CSF threshold.

6 References

AlKheder, S. and Almusalam, A.: Forecasting of carbon dioxide emissions from power plants in Kuwait using United States Environmental Protection Agency, Intergovernmental panel on climate change, and machine learning methods, Renewable Energy, 191, 819-827, https://doi.org/10.1016/j.renene.2022.04.023, 2022.

Hoesly, R., Smith, S. J., Prime, N., Ahsan, H., Suchyta, H., O'Rourke, P., Crippa, M., Klimont, Z., Guizzardi, D., Behrendt, J., Feng, L., Harkins, C., McDonald, B., Mott, A., McDuffie, A., Nicholson, M., & Wang, S.: CEDS v_2024_07_08 Release Emission Data (v_2024_07_08) [Data set]. Zenodo. https://doi.org/10.5281/zenodo.12803197, 2024.

Hoesly, R., Smith, S. J., Ahsan, H., Prime, N., O'Rourke, P., Crippa, M., Klimont, Z., Guizzardi, D., Feng, L., Harkins, C., McDonald, B., & Wang, S.: CEDS v_2025_03_18 Aggregate Data (v 2025_03_18) [Data set]. Zenodo. https://doi.org/10.5281/zenodo.15059443, 2025.

Krings, T., Gerilowski, K., Buchwitz, M., Hartmann, J., Sachs, T., Erzinger, J., Burrows, J. P., & Bovensmann, H.: Quantification of methane emission rates from coal mine ventilation shafts using airborne remote sensing data. *Atmospheric Measurement Techniques*, *6*(1), 151–166. https://doi.org/10.5194/amt-6-151-2, 2013.

Krings, T., Gerilowski, K., Buchwitz, M., Reuter, M., Tretner, A., Erzinger, J., Heinze, D., Pflüger, U., Burrows, J. P., & Bovensmann, H.: MAMAP – a new spectrometer system for column-averaged methane and carbon dioxide observations from aircraft: Retrieval algorithm and first inversions for point source emission rates. *Atmospheric Measurement Techniques*, *4*(9), 1735–1758. https://doi.org/10.5194/amt-4-1735-2011, 2011.

Krol, M., van Stratum, B., Anglou, I., and Boersma, K. F.: Evaluating NO_x stack plume emissions using a high-resolution atmospheric chemistry model and satellite-derived NO2 columns, Atmos. Chem. Phys., 24, 8243–8262, https://doi.org/10.5194/acp-24-8243-2024, 2024.

Leguijt, G., Maasakkers, J. D., Denier van der Gon, H. A. C., Segers, A. J., Borsdorff, T., and Aben, I.: Quantification of carbon moNO_xide emissions from African cities using TROPOMI, Atmos. Chem. Phys., 23, 8899–8919, https://doi.org/10.5194/acp-23-8899-2023, 2023.

Leguijt, G., Maasakkers, J. D., Denier van der Gon, H. A. C., Segers, A. J., Borsdorff, T., van der Velde, I. R., and Aben, I.: Comparing space-based to reported carbon moNO_xide emission estimates for Europe's iron and steel plants, Atmos. Chem. Phys., 25, 555–574, https://doi.org/10.5194/acp-25-555-2025, 2025.

Martínez-Alonso, S., J. Veefkind, B. Dix, B. Gaubert, N. Theys, et al. S-5P/TROPOMI-Derived NO_x Emissions from Copper/Cobalt Mining and Other Industrial Activities in the Copperbelt (Democratic Republic of Congo and Zambia). Geophysical Research Letters, 50 (19), pp.e2023GL104109.ff10.1029/2023GL104109ff. ffhal-04794013f, 2023.

Meier, S., Koene, E. F. M., Krol, M., Brunner, D., Damm, A., and Kuhlmann, G.: A lightweight NO2-to-NO $_{\rm X}$ conversion model for quantifying NO $_{\rm X}$ emissions of point sources from NO2 satellite observations, Atmos. Chem. Phys., 24, 7667–7686, https://doi.org/10.5194/acp-24-7667-2024, 2024.

MoE/UNDP/GEF. Lebanon's Fourth Biennial Update Report the UNFCCC, available at: https://unfccc.int/sites/default/files/resource/Lebanon%20BUR4%202021.pdf, 2021.

Muyemeki, L., Burger, R., Piketh, S.J., Language, B., Beukes, J.P. & van Zyl, P.G. Source apportionment of ambient PM10-25 and PM2.5 for the Vaal Triangle, South Africa. South African Journal of Science, 117(5-6), 1-11. https://doi.org/10.17159/sajs.2021/8617, 2021.

Sadavarte, P., Pandey, S., Maasakkers, J. D., Lorente, A., Borsdorff, T., Denier Van Der Gon, H., Houweling, S., & Aben, I.: Methane Emissions from Superemitting Coal Mines in Australia

Quantified Using TROPOMI Satellite Observations. *Environmental Science & Technology*, 55(24), 16573–16580. https://doi.org/10.1021/acs.est.1c03976, 2021.

Schooling, C. N., Palmer, P. I., Visser, A., and Bousserez, N.: Development of a parametrised atmospheric NO_x chemistry scheme to help quantify fossil fuel CO2 emission estimates, EGUsphere [preprint], https://doi.org/10.5194/egusphere-2024-3949, 2025.

Tian, Y., Sun, Y., Borsdorff, T., Liu, C., Liu, T., Zhu, Y., Yin, H., & Landgraf, J.: Quantifying CO emission rates of industrial point sources from Tropospheric Monitoring Instrument observations. *Environmental Research Letters*, *17*(1), 014057. https://doi.org/10.1088/1748-9326/ac3b1a, 2022.

Triani, M., Dewi, K., Sitanggang, R., Cahyo, N., Rasgianti, R., Supriyanto, E., Bakti, D., Vincēviča-Gaile, Z. Development of Emission Factors from Indonesian Coal-Fired Power Plant Using Continuous Emission Monitoring Data, BIO Web of Conferences 104, 00025 (2024), https://doi.org/10.1051/bioconf/202410400025, 2024.

Varon, D. J., Jacob, D. J., Jervis, D., & McKeever, J.: Quantifying Time-Averaged Methane Emissions from Individual Coal Mine Vents with GHGSat-D Satellite Observations. *Environmental Science & Technology*, *54*(16), 10246–10253. https://doi.org/10.1021/acs.est.0c01213, 2020.

Varon, D. J., Jacob, D. J., McKeever, J., Jervis, D., Durak, B. O. A., Xia, Y., & Huang, Y.: Quantifying methane point sources from fine-scale satellite observations of atmospheric methane plumes. *Atmospheric Measurement Techniques*, *11*(10), 5673–5686. https://doi.org/10.5194/amt-11-5673-2018, 2018.

Document History

Version	Author(s)	Date	Changes
1.0	Marc Guevara ¹ , Oscar Collado ¹ , Gerrit Kuhlmann ² , Erik Koene ² , Stijn Dellaert ³ , Claire van der Wal ³ , Hugo Denier van der Gon ³ ¹ BSC ² EMPA ³ TNO	18/07/2025	First version
1.1	Marc Guevara ¹ , Oscar Collado ¹ , Gerrit Kuhlmann ² , Erik Koene ² , Stijn Dellaert ³ , Claire van der Wal ³ , Hugo Denier van der Gon ³ ¹ BSC ² EMPA ³ TNO	31/07/2025	Addressed minor comments from internal reviewer

Internal Review History

Internal Reviewers	Date	Comments
Frederic Chevallier (CEA)	July 2025	